Dictyostelium discoideum vegetative cells DNA extracellular traps induced by different stimuli: A comparative analysis.

Tesis

Entregada A La
Universidad De Chile
En Cumplimiento Parcial De Los Requisitos
Para Optar Al Grado De

Magíster en Ciencias Biológicas

Facultad De Ciencias

Por

Antonia Sofia Ramos Guzmán

Marzo, 2024

Director de Tesis Dr Francisco P. Chavez
Co-director de Tesis Dr Andrés Marcoleta

FACULTAD DE CIENCIAS

UNIVERSIDAD DE CHILE

INFORME DE APROBACION

TESIS DE MAGÍSTER

Se informa a la Escuela de Postgrado de la Facultad de Ciencias que la Tesis de Magister presentada por la candidata.

Antonia Sofia Ramos Guzmán

Ha sido aprobada por la comisión de Evaluación de la tesis como requisito para optar al grado de Magíster en Ciencias Biológicas, en el examen de Defensa Privada de Tesis rendido el día …….

Director de Tesis:
Dr. .....

Co-Director de Tesis
Dr. .....

Comisión de Evaluación de la Tesis

Dr. .....

Dr. .....

Dr. .....
Dr. .....

A mis amistades, mamá y hermano, los amo.

BIOGRAFÍA

Nacida y criada en Estación Central, siempre me gustó el arte al igual que mi mamá, tanto así que pensé que me dedicaría a algo artístico. (Des)afortunadamente en mi adolescencia conocí lo que era un célula y mi fascinación fue tanta que decidí ser científica. Así, entré a estudiar Biología en JGM, lo cual me hizo confirmar mi encanto por el mundo microscópico y también por la investigación. Estoy agradecida de todo lo que la ciencia me ha dado hasta ahora y estoy ansiosa por ver lo que me dará en el futuro.

AGRADECIMIENTOS

Desde que comencé mi tesis hasta ahora muchas cosas han cambiado en mi vida y nunca anticipé lo importante que iba a ser una ameba en ella. Quiero agradecer a mis amigas y amigos que siempre me han apoyado. Desde el liceo, Cartu, Javi y Alvaro: su perseverancia, resiliencia y pasión por sus proyectos siempre me ha inspirado. A mis compañeros de licenciatura, haber compartido con ustedes durante cuatro años fue un real privilegio, especialmente cuando la mitad de la carrera fue por Discord durante la pandemia. Quiero agradecer particularmente a Valeish, Pelao, Gabo y Maijara, son los mejores. A mis compañeros de Sysmicro y el BEM, la tesis no se hubiera logrado sin ustedes, el apoyo técnico y emocional cada vez que los experimentos salían mal es invaluable, cada almuerzo con ustedes siempre alegró el día. Mención especial a los miembros de Pam's office Mati y Pauli por todo su apoyo y a Camilo, Jose, Ian y Amelia por aguantar mis delirios dentro y fuera del laboratorio. Agradecimiento especial a mi co-tutor Andrés Marcoleta por todo su apoyo, su rigor contribuye a la confianza que tengo en mi trabajo. Agradecimiento muy especial a Francisco Chávez quien me permitió entrar a su laboratorio sin ninguna experiencia al final del pregrado y ha sido primordial en mi carrera científica. Chávez no solo ha confiado más en mi que yo misma, sino que además me dió la oportunidad de ir a Londres a investigar, lo cual sinceramente cambió mi vida. Por último, agradecer con todo mi corazón a mi hermano y a mi mamá. Gracias por fingir entender lo que les contaba de la tesis y por siempre apoyarme en mis decisiones y ambiciones, los amo.

INDEX

LIST OF TABLES

LIST OF SUPPLEMENTARY TABLES

LIST OF FIGURES

LIST OF SUPPLEMENTARY FIGURES

LIST OF SYMBOLS, ABBREVIATIONS OR NOMENCLATURE

AggNETs: Aggregative Neutrophil Extracellular Traps

DAG: diacylglycerol

DNA: Deoxyribonucleic acid

ET: Extracellular Trap

GFP: Green Fluoresce Protein

LPS: Lipopolysaccharide

MPO: Myeloperoxidase

mtDNA: Mitochondrial DNA

NADPH: Nicotinamide adenine dinucleotide phosphate

NE: Neutrophil Elastase

NETs: Neutrophil Extracellular Traps

PAMPs: Pathogen-associated molecular patterns

PCR: Polymerase chain reaction

PKC: Protein Kinase C

PMA: Phorbol 12-myristate 13-acetate

qPCR: Quantitative Polymerase chain reaction

ROI: Region of Interest

ROS: Reactive Oxygen Species

RESUMEN

Dictyostelium discoideum es una ameba social versátil que en su ciclo de vida exhibe tanto etapas multicelulares como unicelulares, según las condiciones ambientales. Entre otras características, ha sido ampliamente utilizada como organismo modelo para el estudio de diversos procesos celulares, incluidos aquellos asociados con la inmunidad innata. Recientemente, las células centinela (células S) de su fase babosa multicelular han demostrado la capacidad de realizar ETosis, un proceso observado inicialmente en neutrófilos. La ETosis implica la liberación de ADN, formando trampas extracelulares (ETs) utilizadas para retener y neutralizar patógenos. Estudios previos realizados por nuestro grupo de investigación mostraron que la ETosis también ocurre en células vegetativas de *D. discoideum* después de la estimulación con diversas cepas bacterianas, no obstante, se desconoce cuáles serían las señales moleculares que inducen la producción de ETs, la naturaleza específica del ADN liberado, y las proteínas asociadas.

En este estudio, empleamos lipopolisacáridos (LPS) de *Klebsiella pneumoniae (K. pneumoniae)* y *Salmonella enterica (S. enterica)* para caracterizar la liberación de ETs, estableciendo un modelo fundamental para estudiar este proceso en células vegetativas de *D. discoideum*. Utilizando imagenología de células vivas, observamos ETs en células individuales y poblaciones celulares, revelando similitudes estructurales y dinámicas con células del sistema inmune como neutrófilos de mamíferos. Además, mediante qPCR, identificamos un aumento significativo en la secreción de ADN mitocondrial después de la estimulación con LPS de ambas cepas bacterianas. Por otra parte, desarrollamos una estrategia basada en proteómica cuantitativa para evaluar la presencia y abundancia relativa

de proteínas asociadas a ETs de células vegetativas de *D. discoideum* inducidas por LPS de *K. pneumoniae*. Los resultados evidenciaron un aumento en la cantidad de proteínas asociadas a ETs durante su inducción. Un análisis de expresión diferencial identificó numerosas proteínas con funciones desconocidas en comparación con las células no inducidas. Además, dos proteínas de la familia de deshidrogenasa/reductasa de cadena corta fueron enriquecidas tras la estimulación.

Estos hallazgos no solo ofrecen conocimientos valiosos sobre los mecanismos de la ETosis en *D. discoideum*, sino que también lo posicionan como un modelo prometedor de célula inmune para estudiar la producción de ETs. Esta investigación sienta las bases para futuros estudios sobre las proteínas y las vías específicas involucradas en la ETosis de *D. discoideum*, brindando una perspectiva única sobre los mecanismos de defensa antimicrobiana y la inmunidad innata.

ABSTRACT

Dictyostelium discoideum is a versatile social amoeba that, in its life cycle, exhibits both multicellular and unicellular stages depending on environmental conditions. Among other characteristics, it has been widely utilized as a model organism for the study of various cellular processes, including those associated with innate immunity. Recently, sentinel cells (S cells) from the multicellular slug phase have demonstrated the ability to undergo ETosis, a process initially observed in neutrophils. ETosis involves the release of DNA, forming extracellular traps (ETs) used to entrap and neutralize pathogens. Previous studies conducted by our research group demonstrated that ETosis also occurs in vegetative cells of *D. discoideum* after stimulation with various bacterial strains. However, the molecular signals inducing ET production, the specific nature of released DNA, and the associated proteins remain unknown.

In this study, we employed lipopolysaccharides (LPS) from *Klebsiella pneumoniae (K. pneumoniae)* and *Salmonella enterica (S. enterica)* to characterize ET release, establishing a foundational model to investigate this process in vegetative cells of *D. discoideum.* We observed ETs at both single-cell and population levels, utilizing live cell imaging, revealing structural and dynamic similarities with immune system cells such as mammalian neutrophils. Furthermore, through qPCR, we identified a significant increase in mitochondrial DNA secretion after LPS stimulation of both bacteria strains. Additionally, we developed a strategy based on quantitative proteomics to assess the presence and relative abundance of proteins associated with ETs in vegetative cells of *D. discoideum* induced by *K. pneumoniae* LPS. The results demonstrated an increase in the quantity of proteins

associated with ETs during their induction. Differential expression analysis identified numerous proteins with unknown functions compared to non-induced cells. Additionally, two proteins from the short-chain dehydrogenase/reductase family were enriched upon stimulation.

These findings offer valuable insights into the intricate mechanisms of ETosis in *D. discoideum* and position it as a promising immune cell model for studying ETs production. This research lays the groundwork for future studies on the specific proteins and pathways involved in *D. discoideum* ETosis, offering a unique perspective on antimicrobial defense mechanisms and innate immunity.

1 INTRODUCTION

1.1 Phagocytosis and the origin of immunity

"What's true for Escherichia coli is also true for elephants"

Jacques Monod.

The intricate realm of immune cells, with their multifaceted functions in safeguarding organisms against invaders, has been a captivating subject of exploration throughout scientific history. Élie Metchnikoff, a pivotal figure in this narrative, transitioned from a zoologist to a pathologist, leaving an indelible mark on our understanding of the immune response through his discovery of phagocytosis—a fundamental cellular process (Kaufmann, 2008) .

Metchnikoff's scientific journey began with thoroughly exploring marine organisms' microscopic structures and embryology. His investigations included various organisms such as *Turbelaria* (Metschnikoff, 1878), *Coelenterata* (Metschnikoff, 1880), Starfish larvae (Metschnikoff, 1884a), and even *Daphnia* (Metschnikoff, 1884b). After years of observation and experimentation, he coined the term "phagocyte" for cells capable of uptaking external particles and attacking foreign material, in a process named "phagocytosis." Metchnikoff seamlessly integrated Haeckel's evolutionary concepts into his studies, providing a broader context for exploring the intricacies of immune processes. Additionally, he was influenced by Koch's identification of bacterial pathogens within host cells, incorporating these insights into his investigations of cellular defense mechanisms (Kaufmann, 2008).

Metchnikoff's findings were revolutionary, and his visionary concept extended beyond nutritional activity, foreseeing broader implications for host defense mechanisms. This pioneering work laid the foundation for our comprehensive knowledge of immune cells and phagocytosis (Kaufmann, 2008).

In contemporary times, the scope of phagocytosis extends beyond the animal kingdom, encompassing various organisms, including the protozoan social amoeba *Dictyostelium discoideum*, now acknowledged as a professional phagocyte (Clarke & Maddera, 2006). Metchnikoff's evolutionary approach to research serves as the cornerstone for investigations with model organisms in the field of immunology. Remarkably, the initial exploration in this realm did not focus on humans or mammals. Nevertheless, the universality of phagocytosis observed in invertebrate marine organisms appears to hold true for humans—a phenomenon reminiscent of Monod's famous quote.

1.2 *Dictyostellium discoideum* as an immune cell model

Social amoebas, an intriguing group of microorganisms thriving in soil ecosystems, sustain themselves by feeding on bacteria, boasting a global diversity of more than 150 identified species (Escalante & Cardenal-Muñoz, 2019). One of these species is *Dictyostelium discoideum*, which was initially discovered in 1933 in the Craggy Mountains of Western North Carolina (Raper KB, 1935).

This organism exhibits a dual life cycle (Figure 1), transitioning between unicellular and multicellular stages based on environmental conditions (Brock et al., 2016). During its unicellular phase, *D. discoideum* actively engages in phagocytosis to engulf bacteria and yeasts (Mathavarajah et al., 2017). However, in conditions of food scarcity, it enters a

multicellular social stage initiated by cell aggregation. Subsequently, this aggregate transforms into a motile slug, moving towards heat and light. Following the slug phase, a culmination phase occurs, resulting in the formation of a fruiting body with a spore-filled head that is then released, initiating a transition back to vegetative cells and the commencement of a new cycle. The feeding behavior of vegetative cells closely mirrors the phagocytic behavior observed in mammalian professional phagocytes (Bozzaro et al., 2008) Notably, beyond phagocytosis, *Dictyostelium discoideum* exhibits further similarities to immune cells, showcasing capabilities such as micropinocytosis (Junemann et al., 2016) and chemotaxis (Scavello et al., 2017).

Beyond its biological characteristics, *D. discoideum* also offers a range of experimental advantages. It can be easily cultivated in axenic media and requires relatively simple equipment for maintenance (Dunn et al., 2018). Moreover, its haploid nature renders it highly amenable to genetic manipulation (Steinert & Heuner, 2005) and it has a comprehensive database where mutant strains and experimental protocols can be found (Kreppel et al., 2004). Consequently, *D. discoideum* has emerged as an exceptional model for investigating various aspects of development and other biological processes relevant to innate immunity (Dunn et al., 2018).

Recent research has revealed that, besides the previously mentioned immune-like characteristics, *D. discoideum* can also produce DNA extracellular traps (ETs) (Zhang et al., 2016). This process, first discovered in neutrophils (Brinkmann et al., 2004), appears to play a beneficial role in host defense mechanisms (Kaplan & Radic, 2012). This phenomenon was observed in S cells from the multicellular slug phase of *D. discoideum* (Figure 1). However, limited information exists regarding the occurrence of this process in the vegetative cells of this organism.

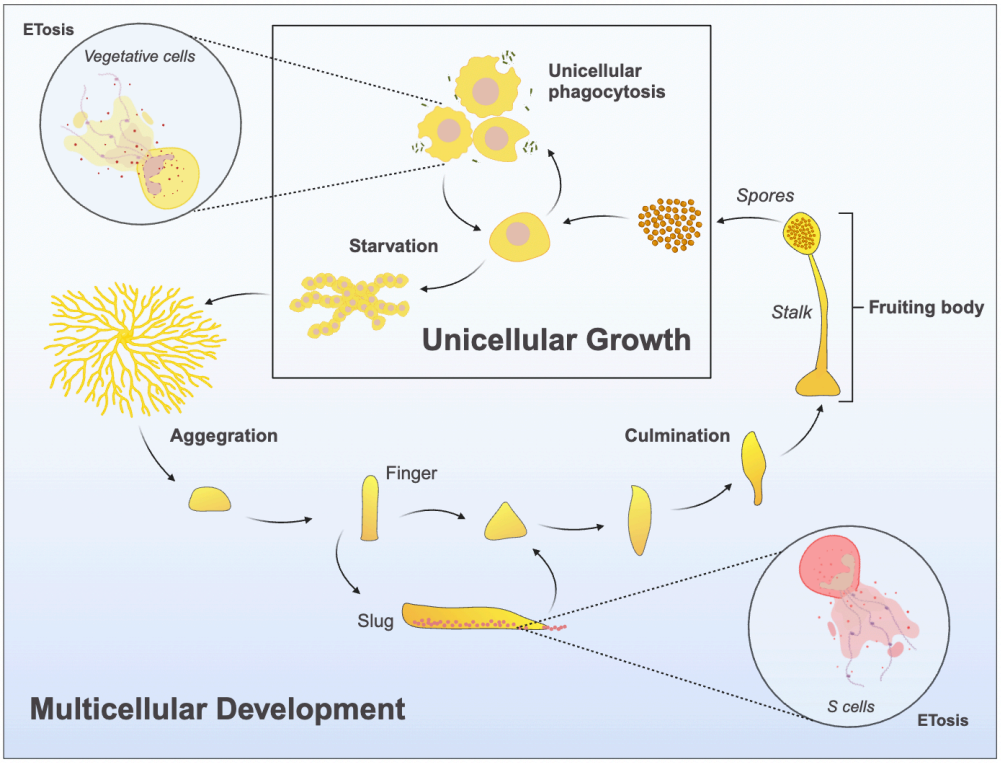

Figure 1. *Dictyostelium discoideum* Life Cycle. The life cycle commences with spores released by the fruiting body, developing into vegetative cells that sustain themselves through phagocytosis. As our group shows, these professional phagocytes can undergo ETosis when encountering specific bacteria and Lipopolysaccharide (LPS). As the food supply diminishes, triggering a starvation phase, vegetative cells initiate the aggregation process, forming larger multicellular structures, one referred to as the "slug." During this multicellular phase, specialized Sentinel cells (S cells) within the slug also demonstrate the capacity for ETosis in the presence of certain bacteria and LPS (Zhang et al., 2016). Following the slug phase, a culmination phase ensues, forming a fruiting body characterized by a stalk and spore-filled head. This marks the restart of the cycle. Created with BioRender.com

1.3 DNA Extracellular Traps

1.3.1 From NETosis to ETosis

Neutrophil Extracellular Traps (NETs) are web-like structures made up of anti-microbial proteins and the neutrophil's nuclear DNA (Kenny et al., 2017) and play a pivotal

role in immobilizing and neutralizing bacteria (Brinkmann & Zychlinsky, 2012). The active process of producing NETs, termed NETosis, was initially identified as triggered by phorbol 12-myristate 13-acetate (PMA), Gram-positive and Gram-negative bacteria, and Lipopolysaccharide (LPS). Further exploration into NETs unveiled their efficiency against eukaryotic pathogens, particularly *Candida Albicans* (Urban et al., 2006). Notably, NETs exhibit pathogen-disarming capabilities, employing proteases and antimicrobial activity from the histones within the structures (Brinkmann et al., 2004).

Subsequent studies elucidated the mechanism of NETosis, affirming its unique and distinct nature separate from necrosis and apoptosis (Fuchs et al., 2007). Unlike apoptosis, NETosis does not exhibit DNA fragmentation or phosphatidylserine exposure, typical features of programmed cell death. Additionally, an absence of membrane fragmentation—a characteristic trait of necrosis and apoptosis—further delineates NETosis as a unique process (Goldmann & Medina, 2012).

Beyond neutrophils, mast cells have emerged as another immune cell capable of producing these structures (Von Köckritz-Blickwede et al., 2008) Subsequent advancements uncovered that besides mammalian immune cells, invertebrate immune cells were also capable of undergoing this process (Homa et al., 2016; Ng et al., 2013; Robb et al., 2014). The scope was broadened even further in the following years, extending beyond the animal kingdom. A comprehensive review has posited ETosis as an ancient defense mechanism across multiple kingdoms, substantiating its prevalence in multiple species (Neumann et al., 2020), which includes the social amoeba *Dictyostelium discoideum.*

These cumulative findings prompted the adoption of the term "ETosis" in place of "NETosis," recognizing that various immune cells, not just neutrophils, can undergo this process (Goldmann & Medina, 2012). This shift in terminology sparked an exploration into

the spectrum of cells capable of producing ETs, alongside investigations into the stimuli and mechanisms triggering this phenomenon, and its correlation with inflammatory processes and illnesses (Bonaventura et al., 2020; Nakazawa et al., 2018; Porto & Stein, 2016; Poto et al., 2022).

1.3.2 The mechanism of Extracellular Traps formation

The specifics regarding the pathways contributing to the formation of extracellular traps (ETs) (Goldmann & Medina, 2012) and even neutrophil extracellular traps (NETs) (Bronkhorst et al., 2022) remain subjects of controversy and ongoing debate. This controversy arises from recognizing that ET formation can proceed through multiple pathways depending on the stimuli employed (Kenny et al., 2017; Neumann et al., 2020) and that the DNA released in ETs does not always originate from the nucleus but can also come from mitochondria. In contrast to the initial findings reported in neutrophils, eosinophils can produce ETs composed of mitochondrial DNA (mtDNA), presenting an alternative and novel mechanism (Yousefi et al., 2008). Furthermore, the same research group subsequently discovered mtDNA ETs in neutrophils as well (Yousefi et al., 2009) indicating that neutrophils possess the capability for both mitochondrial and nuclear DNA ET formation. This suggests that there may be two distinct processes depending on the source of DNA (Yousefi et al., 2019). Despite these controversies, two main types have been described: suicidal and vital ETosis.

Suicidal ETosis, initially observed in neutrophils, involves a sequential cascade of events. Protein kinase C (PKC) activates NADPH oxidase upon stimulation, generating ROS (Cubillo-Martínez et al., 2022). Subsequently, myeloperoxidase (MPO) is stimulated, activating and translocating neutrophil elastase (NE) from specialized vesicles to the nucleus.

Within the nucleus, MPO, NE (Papayannopoulos et al., 2010) and other enzymes (Y. Wang et al., 2009)collaboratively decondense chromatin. After this process, the nuclear envelope disassembles, and the decondensed nuclear chromatin is released into the cytoplasm, which merges with cytoplasmic and granule components. Approximately 3 hours post-activation, NETs are extruded into the extracellular space following membrane rupture and subsequent cell death (Fuchs et al., 2007; Papayannopoulos, 2018).

In contrast, Vital ETosis operates without necessitating cell death. An intriguing mechanism has been elucidated in neutrophils, both *in vitro* and *in vivo*, wherein nuclear DNA is released in vesicles through blebbing directly from the nucleus. Importantly, the nuclear and plasma membranes remain initially intact, thereby preserving cellular viability (Pilsczek et al., 2010; Yipp et al., 2012).

An alternative form of vital ETosis involves the expulsion of mtDNA and requires ROS. This phenomenon has been observed not only in eosinophils and neutrophils (Yousefi et al., 2008, 2009) but also in basophils (Morshed et al., 2014) and S cells from the *D. discoideum* slug phase (Zhang et al., 2016). Regarding the reported extrusion mechanisms, mtDNA can be released into the cytosol, where it is subsequently encapsulated into vesicles. These vesicles are then released through fusion with the plasma membrane, forming traps (Conceição-Silva et al., 2021). Alternatively, mtDNA can be directly expelled in a catapult-like manner through the fusion of the mitochondrial and plasma membranes (Conceição-Silva et al., 2021; Yousefi et al., 2008, 2009, 2019).

It is noteworthy that the release of mtDNA has been observed in S cells of *D. discoideum* when exposed to *K. pneumoniae* and its LPS (Figure 1). While the precise mechanism of ETosis in these cells is not fully elucidated, it has been established that TIR domain-containing proteins serve as signal transducers for the LPS stimulus. Additionally,

the process involves the utilization of NADPH oxidases for the generation of ROS, which are further employed as signaling molecules to initiate ETosis (Zhang et al., 2016).

1.3.3 Extracellular Traps appearance

When ETs were initially characterized in neutrophils, they were described as extracellular fibers composed of nuclear and granule components (Brinkmann et al., 2004). Subsequent studies have revealed that the appearance of ETs can vary depending on different factors. A recent review has categorized different NETs based on their appearance, showcasing variations such as the prevalent "Cloudy NETs" or "Spiky NETs." The visual characteristics of these NETs are primarily influenced by the stimuli applied (Daniel et al., 2019). Interestingly, similar structures have also been observed in non-mammalian immune cells, specifically in hyaline cells from *C. maenas* that also present ETs aggregation structures (Robb et al., 2014). This distinct type, termed "Aggregated NETs" (AggNETs) in neutrophils, tends to appear at higher cell densities in both *in vitro* and *in vivo* settings (Schauer et al., 2014) and can be induced by soluble ligands such as LPS. AggNETs often contain neutrophils that have not undergone NETosis, debris, epithelial cells, bacteria, and enzymes that contribute to pathogen clearance (J. Hahn et al., 2016 ; Daniel et al., 2019).

ETs have also been observed in coelomocytes, immunocompetent cells found in earthworms. Coelomocytes, responsible for various immune functions like phagocytosis, cytotoxicity, and secretion of humoral factors, are interestingly classified into amoebocytes and eleocytes (Homa, 2018). ETs have been identified in both types of coelomocytes, presenting a spiky-like structure and aggregated forms (Homa et al., 2016). This research also emphasizes how the appearance of ETs changes throughout the different stages of

formation, ranging from a small amount of DNA extruding from the cell to the cell being fully covered in DNA.

While not explicitly reported for S cells of *D. discoideum*, it is noteworthy that their ET appearance resembles smaller, spiky-like ET structures and aggregates (Zhang et al., 2016). The reduced size of the ET structure in S cells can be attributed to the source of DNA, originating from the mitochondria rather than the nucleus. The discernible contrast in mtDNA abundance compared to nuclear DNA likely contributes to forming a smaller ET structure in S cells.

Hence, the specific appearance of ETs varies depending on the cell type undergoing the process, the stimulus employed, cell concentration, and even the origin of the DNA released. Moreover, the involvement of proteases in damaging captured microbes can also play a role in shaping the structure of ET chromatin (Kaplan & Radic, 2012).

1.3.4 Proteins associated with Extracellular Traps

The initial exploration of ETs involved immunofluorescent techniques, identifying potential proteins present and subsequently seeking them out (Brinkmann et al., 2004). However, recent investigations have shifted focus towards a comprehensive proteomic analysis, particularly determining the ET proteome using bottom-up proteomics through liquid chromatography-tandem mass spectrometry (LC-MS/MS) (Urban et al., 2009)(Chapman et al., 2019)(Petretto et al., 2019)(Scieszka et al., 2022). Consequently, researchers have attempted to isolate proteins associated with ETs. This endeavor poses challenges, as the distinction between ET proteins and the secretome cannot be entirely ensured, considering the most popular protocols used for ET protein isolation. Common to all protocols is the reliance on nuclease treatment to detach proteins physically linked to the

DNA of ETs. Supplementary Table 1 summarizes the four most cited proteomic protocols regarding NETs. All these four protocols have been conducted in neutrophils, and there is limited information regarding the ET proteome in other cell types.

The primary proteins secreted in most ETosis processes include defensins, histones (Goldmann & Medina, 2012) and other proteins with antimicrobial activity (Kaplan & Radic, 2012). Furthermore, broad-spectrum antimicrobial peptides have been identified (Von Köckritz-Blickwede et al., 2008). It is essential to emphasize that the precise proteomic profile of these extracellular traps is highly contingent on the nature of the inducer employed (Petretto et al., 2019; Chapman et al., 2019).

1.3.5 Stimuli triggering Extracellular Trap production.

Various inducers have been identified to stimulate the formation of ETs in diverse cell types (Daniel et al., 2019; Goldmann & Medina, 2012; Guimarães-Costa et al., 2012). The impact of these inducers on the ETosis process is not only dictated by their chemical nature but also influenced by their concentration (Hoppenbrouwers et al., 2017) and time of exposure (Scieszka et al., 2022) leading researchers to employ varied experimental settings, even within studies involving the same cell type (Naccache & Fernandes, 2016).

NETosis has been primarily examined in response to PMA, a potent mitogen and a robust NET inducer (Kenny et al., 2017). Other non-biological inducers include bicarbonate (Leppkes et al., 2016), calcium ionophore (Kenny et al., 2017), and even monosodium urate microcrystals (Schorn et al., 2012). Biological inducers encompass fungi (Urban et al., 2009), viruses (Zhu et al., 2018), and Gram-positive and Gram-negative bacteria (Goldmann & Medina, 2012; Von Köckritz-Blickwede et al., 2008). Lipopolysaccharides have also been a widely utilized ET inducer since the early reports of NETs, making them key inducers of this

phenomenon (Brinkmann et al., 2004). LPS are integral components within the membranes of gram-negative bacteria (Liu et al., 2016) and comprise three distinct structural domains: lipid A, the core oligosaccharide, and the O antigen (O-Ag). Lipid A serves as the anchor, tethering LPS to the outer membrane, and is primarily responsible for its toxic effects. Within the core structure, there are both internal and external regions, with the external portion hosting the O-Ag, consisting of repetitive units of oligosaccharides (Raetz & Whitfield, 2002; Rietschel et al., 1994). While lipid A and the core remain highly conserved among Enterobacteriaceae species the O-Ag exhibits significant variability in sugar composition, arrangement, and polymerization degree (Caroff & Karibian, 2003). This variability in the O-Ag confers diverse antigenic properties to different bacterial strains and plays a pivotal role in virulence, serving as the frontline interface between the bacterium and its host (Wang Xiaoyuan & Quinn Peter J., 2010).

Considering the complexity of these molecules, it has been reported that neutrophils exhibit a remarkable ability to differentiate between LPS from various bacterial species, selectively releasing NETs (Pieterse et al., 2016). Moreover, S cells of *D. discoideum* have also been observed to produce ETs when exposed to LPS, specifically derived from *K. pneumoniae* (Zhang et al., 2016). Although *K. pneumoniae* LPS typically demonstrates limited serotype diversity in its O-Ag, based on the glycan composition and structure of the O-Ag repeating units (Vinogradov et al., 2002), other Enterobacteriaceae species such as *S. enterica* exhibit a broader range of O-Ag forms, including short, long, and very long forms with varying numbers of repeats (Zenk et al., 2009).

Interestingly, in prior research, our group extensively explored the interactions between the bacterial pathogens *K. pneumoniae* and *S. enterica* with *D. discoideum*

(Hernández et al., 2023; Marcoleta et al., 2018; Varas et al., 2018). This work validated the social amoeba as a model for studying resistance to phagocytosis and intracellular survival.

Based on this evidence, there is a compelling motivation to investigate the effect of *K. pneumoniae* and *S. enterica* LPS as potential inducers of ETosis in vegetative cells of *D. discoideum*, especially considering their differences which may elucidate differential responses in ETosis, akin to observations in neutrophils.

1.4 *Dictyostelium discoideum* Vegetative Cells Extracellular traps

According to the evidence described above, *D. discoideum* is as an exceptional model for phagocytosis studies. Furthermore, the recent discovery of ET production in S cells enhances its status as an immune cell model and prompts questions about the potential engagement of vegetative cells in ETosis. In this regard, it is reasonable to consider whether this process occurs to enhance survival in its singular cell state, similar to what is seen in mammalian immune cells. Our laboratory explored this inquiry, investigating whether vegetative cells can generate DNA extracellular traps. According to live cell imaging experiments, these cells release DNA when induced by different bacterial strains. Intriguingly, discernible DNA secretion is observed even without external induction (Farías-Moreno & Chavez Espinosa, 2021).

The revelation of DNA secretion prompts fundamental questions about its nature. Building upon the precedent set by S cells, the inquiry arises: do vegetative cells also secrete mtDNA in ETs? If not, the possibility of suicidal ETosis (nuclear ETs) arises, given the altruistic behavioral traits exhibited by *D. Discoideum* (Atzmony et al., 1997). On the contrary, if vegetative cells mainly secrete mtDNA, it becomes intriguing to investigate the

frequency of cells engaging in ETosis, the aspect of the resulting ETs, and whether they form aggregates akin to those observed in other immune cell types, given the natural aggregation behavior of *D. discoideum* throughout its life cycle (Dormann et al., 2002) .

Furthermore, investigations into various cell types producing ETs have unveiled distinct sources of DNA (Goldmann & Medina, 2012) and proteomic profiles within these ETs (Chapman et al., 2019; Petretto et al., 2019), influenced by the type of stimulus. Consequently, unraveling the proteomic content and DNA nature of ETs induced by different stimuli may provide insights into the diverse responses of *D. discoideum.* Given the amoeba's discernible variations in response to different strains during phagocytosis (Nasser et al., 2013) and neutrophils' ability to discriminate between LPS in ET release (Pieterse et al., 2016), it is plausible that the proteomic composition and DNA nature of ETs may exhibit analogous differential responses.

Given the background presented in this section, the primary objective of this thesis is to comprehensively characterize ETosis in vegetative cells of the professional phagocyte *Dictyostelium discoideum*, shedding light on the intricacies of this phenomenon. In particular, we focused on Pathogen associated molecular patterns (PAMPs), specifically emphasizing LPS instead of employing entire pathogens. This deliberate approach ensures that pathogen-derived DNA or proteins do not interfere with the analysis. The decision to use LPS extracted from *K. pneumoniae* and *S. enterica* was driven by our laboratory's prior research involving these strains and *D. discoideum*, establishing a relevant context for our investigations.

1.4 Hypothesis

Extracellular traps produced by *Dictyostelium discoideum* vegetative cells will differ in their proteomic profile and DNA composition upon induction by LPS from *K. pneumoniae* and *S. enterica*.

1.5 Objectives

1.5.1 Main Objective

To compare the global proteomic profiles of ETs and their DNA composition produced by *D. discoideum* vegetative cells in response to LPS from *K. pneumoniae* and *S. enterica*.

1.5.2 Specific Objective

1. To compare ET dynamics at a population and single-cell level in response to *K. pneumoniae* and *S. enterica* LPS.
2. To determine the DNA composition of ETs in response to *K. pneumoniae* and *S. enterica* LPS.
3. To compare the global proteomic profile of ETs in response to *K. pneumoniae* LPS stimulation.

2 MATERIALS AND METHODS

2.1 Reagents, media and buffers

The reagents, media, and buffers used in this study are listed in Table 1 and Table 2. Table 1 details the sources and identifiers for the reagents, while Table 2 outlines the compositions of the media and buffers employed.

Table 1. Reagent List

Reagent	Source
Lipopolysaccharide from *Klebsiella pneumoniae* (ATCC 15380)	Sigma-Aldrich – L4268
Lipopolysaccharide from *Salmonella enterica* (ATCC 10749)	Sigma-Aldrich – L6386
Phorbol 12-myristate 13-acetate (PMA)	Sigma-Aldrich – P8139
Sytox Green	Invitrogen- S7020
Turbo DNAse	Invitrogen - AM2238
Master Mix q-PCR	Bio-Rad - 1725270
EDTA	Sigma-Aldrich – ED

Table 2. Media and buffer list

Media / buffer	Content
HL5	14 g/L of tryptone, 7 g/L of yeast extract, 0.35 g/L of Na_2HPO_4, 1.2 g/L of KH_2PO_4, and 14 g/L of glucose, pH 6.3

Sorensen buffer	2.0 g/L KH_2PO_4, 0.29 g/L Na_2HPO_4, pH 6.0 ± 0.1
HotSHOT – Alkaline lysis reagent	25 mM NaOH, 0.2 mM disodium EDTA, pH 12
HotSHOT – Neutralizing Solution	40 mM Tris-HCl in water, pH 5
Turbo DNAse buffer	Invitrogen - AM8170G

2.2 *D. discoideum* strains and culture conditions

Dictyostelium discoideum AX2 (or AX4) axenic strain frozen aliquots were thawed and deposited into Petri dishes containing 11 mL of HL5 medium. The cells were allowed to adhere to the plate surface for about an hour, after which the HL5 medium was removed and replaced with 12 mL of fresh media. The cells were grown until they reached between 90-100% confluence, at which point they were split into different plates with varying cell concentrations depending on the number of cells required and the timing of the experiment. To detach the cells from the plate, a 10 mL serological pipette was used, employing an "up and down" motion until most of the cells were floating in the media. A fresh frozen aliquot was used every 2 weeks, ensuring that sub-cultivation and handling were limited to no more than 5-6 times.

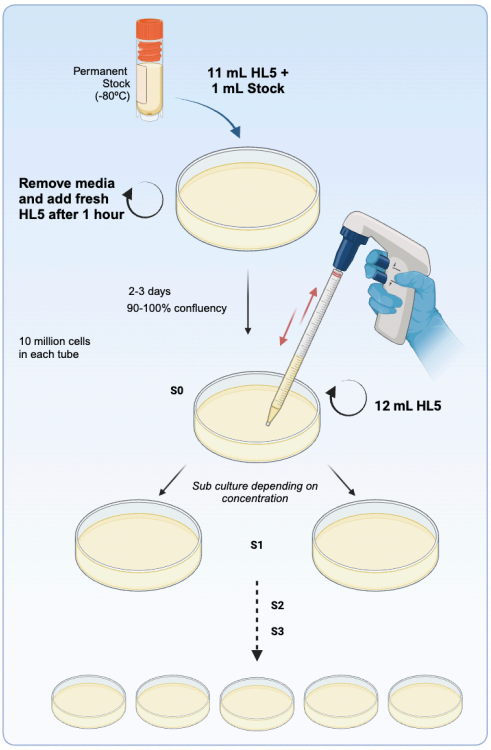

Figure 2. Graphical representation of *D. discoideum* cell culture.

2.3 Microplate assays to evaluate ET production

Different concentrations of ET inducers were tested in *D. discoideum*. We employed LPS from *K. pneumoniae* and *S. enterica* and PMA in both AX2 and AX4 strains. Cells were seeded (2×10^5 cells/200 µL) in 96-well black plates in Sorensen buffer in the presence of 5 µM Sytox Green Nucleic Acid Stain, a non-cell-permeable DNA binding dye for 20 min at 23°C. Cells were then stimulated with 2.5 µg/mL, 5 µg/mL, or 10 µg/mL of each LPS and 30 nM, 40 nM and 50 nM of PMA. Plates were read every 20 min for 4 h on a Tecan microplate reader (infinite 200Pro). Sytox green fluorescence was excited at 480/490 nm and its emission registered at 520 nm. Cells were checked after 4 h in a fluorescent microscope to corroborate that most of them remained alive and that fluorescence came mostly from extracellular DNA.

2.4 Extracellular Trap Visualization through Fluorescent Microscopy

2.4.1 Microplate Imaging

To confirm the presence of extracellular DNA, the microplate previously utilized for microplate reader analysis was subjected to examination using the Lionheart FX automated fluorescence microscope equipped with Gen5 software version 3.14.03 (Agilent). Image acquisition was performed at 20X magnification, utilizing both bright field and green channel settings. Post-capture, the software facilitated image analysis, involving adjustments to brightness and contrast in the fluorescent channel to enhance clarity. For enhanced precision in studying specific phenomena, single fractions were selectively zoomed in when necessary. Subsequently, the acquired images were compiled using Image J version 1.53 (Fiji version). In this compilation, scale bars, arrows, names, and timing details were added for comprehensive documentation.

2.4.2 Extracellular Trap production Kinetics

Cells suspended in Sorensen buffer in the presence of Sytox Green were seeded (3 x10^5 / 300µL) in a 24-well plate and after 20 min they were stimulated with 10µg/mL of each LPS. Images were captured every 10 min at 20X magnification, utilizing bright field and green fluorescence channels.

Each experimental condition was performed and imaged in triplicate, with a region of interest (ROI) selected at the exact center of the plate. A montage setting was applied, capturing four images at the specified magnification around the selected ROI. This approach

increases the visualization area, increasing the likelihood of observing the phenomena and enabling a broader cell population recording.

Following image capture, the analysis process replicated the procedures detailed in the preceding section. In this instance, the analysis also extended to stitching the montage using the "average" method option, specifically based on the GFP channel, facilitated through the Gen5 software.

2.4.3 DNAse treatment in Extracellular Traps

Cells were seeded (3 x10^5 / 300µL) in a 24-well plate in Sorensen buffer in the presence of Sytox Green and after 20 min they were stimulated with 10µg/mL of each LPS. After 4 h of induction, cells were visualized in the bright field and green channel.

Once an ET was identified, its coordinates (x and y position) were promptly saved. Subsequently, 10 U of Turbo DNAse and 10X DNAse buffer, were added carefully to the wells to avoid disrupting the cells. The plate was left at 23°C. After 40 min, the same cells were recaptured using the same GFP channel settings (intensity, integration, and camera gain).

2.6 qPCR for determination of Extracellular Traps DNA nature

For q-PCR and proteomic analysis, a uniform protocol was implemented (Figure 3). Cells were seeded in Sorensen buffer in a 12-well plate and induced accordingly. Following stimulation, the samples were separated into distinct layers: the upper layer designated as the "secretome," the remaining fraction closer to the cells (treated with DNAse for proteomic analysis and untreated for q-PCR) referred to as the "ET fraction," and the cells partially

attached to the bottom of the well denoted as the "Cell fraction." It is noteworthy that a respective centrifugation step followed each separation to ensure no cells or debris contaminated each fraction. Additionally, it is important to mention that, even in the non-induced condition where ETs are not expected, we refer to this fraction as the "ET fraction" for simplicity, facilitating a clear contrast in the different analyses.

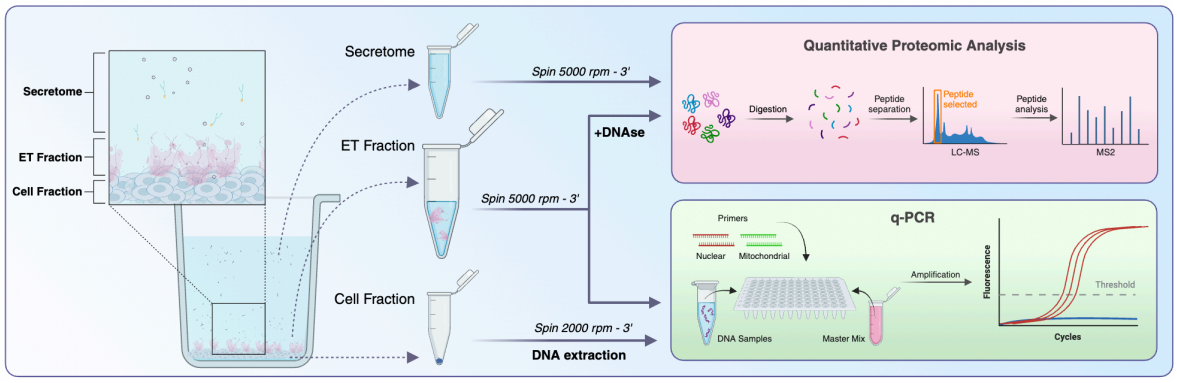

Figure 3. Graphical abstract of sample preparation for qPCR and Proteomic analysis. Following stimulation, the respective sample undergoes separation into distinct layers: the upper layer designated as the "secretome," the remaining fraction closer to the cells treated with DNAse for proteomic analysis referred to as the "ET fraction," and the cells partially attached to the bottom of the well denoted as the "Cell fraction."

2.6.1 Sample preparation

For q-PCR analysis, both the "ET fraction" and the "Cell fraction" were analyzed (figure 3) . Cells were seeded at a density of 4×10^6 cells in 2 mL Sorensen buffer in a 12-well plate and induced with 10 µg/mL of each LPS for 4 h, while the control condition received an equivalent volume of buffer.

The secretome, obtained by carefully aspirating the upper layer (1.5 mL) using a P1000 pipette, was transferred to a clean 15 mL Falcon tube. This fraction was not utilized for q-PCR analysis.

Subsequently, 400 µL of the remaining volume in the plate, comprising the "ET fraction," was collected twice using a P200 pipette from the upper layer, avoiding cell retrieval, and transferred to a 2 mL Eppendorf tube. Centrifugation of this fraction at 5000 rpm for 3 minutes removed any remaining cells or cellular debris, and the resulting supernatant was stored at -20°C for q-PCR analysis.

The remaining cells in the plate, constituting the "cell fraction," were mixed with an additional 100 µL of Sorensen buffer to facilitate cell retrieval. Cell scraping was performed vigorously to detach all cells, and the collected volume was transferred to a 1.5 mL Eppendorf tube. Centrifugation at 2000 rpm for 5 min precipitated the cells; the supernatant was discarded, and the remaining pellet was treated with the HotSHOT method to extract DNA (G.E. Truett et al., 2000). For this, 75 µL of an alkaline lysis reagent was added, pipetting to dissolve the pellet, and then heated at 95°C for 45 min in a PCR tube in a thermocycler. After that time, samples were immediately placed on ice, and 75 µL of the neutralizing solution was added, followed by storage at -20°C until qPCR analysis.

2.6.2 qPCR protocol

Calibration was performed for both nuclear and mitochondrial primers to ensure primer efficiency. Genomic DNA was extracted from *D. discoideum*, and varying quantities of it were used to generate a calibration curve, allowing for the calculation of primer efficiency (Supplementary Figure 3).

qPCR reactions (20 µL) contained SYBR Green Master Mix (Applied Biosystems), 5 µL of sample (ET fraction or HotSHOT prepared pellet), and 500 nM of forward and reverse primers. They were then analyzed in a Bio-Rad CFX96 Touch Real-Time PCR

Detection System employing the CFX Maestro Software version 4.1.2433.1219 with the following parameters modified from another protocol (Lamrabet et al., 2020): 98°C/2 min, 40 cycles of 94°C/10 s, and 60°C/45 s. The cycle threshold (Ct) value of a reaction is defined as the cycle number when the fluorescence of a PCR product can be detected above the background signal. Data were collected from three biological replicates, with three technical replicates for each condition. Negative control reactions were performed, replacing the DNA with nanopure water.

2.6.3 Data and statistical analysis

Data normalization was conducted assuming that all samples originated from an equal number of cells. Primer efficiency was calculated using Equation 1, derived from the calibration curve (Supplementary Figure 3). The Pfaffl method was then applied to determine the ratio between the amounts of mitochondrial DNA against nuclear DNA (Equation 2) using the non-stimulated sample for both ET fraction and cell pellet as control. The average Ct of the three technical replicates was used to calculate the ratio for each of the three biological replicates. Subsequently, an unpaired t-test was employed in Prism software version 9.4.1 to assess the differences between the control and induced conditions ratios for the extracellular trap fraction and the cell pellet fraction separately.

$$E = \left(\frac{\text{Primer efficiency (\%)}}{100}\right) + 1 \qquad \text{Equation 1}$$

$$R = \frac{E(Mitochondrial)^{\Delta\text{Ct target (Control}-\text{Induced)}}}{E(Nuclear)^{\Delta\text{Ct reference(Control}-\text{Induced)}}} \qquad \text{Equation 2}$$

2.5 Quantitative Proteomic Analysis

2.5.1 Sample preparation

For quantitative proteomic analysis, the “ET fraction” together with the “secretome” were analyzed (Figure 3). First, cells were seeded at a density of 4×10^6 cells in 2 mL Sorensen buffer in a 12-well plate and induced with 10 µg/mL of LPS from *K. pneumoniae* for 4 h while the control condition received an equivalent volume of buffer. A total of four wells were prepared for each condition, totaling 16 million cells per condition for subsequent analysis.

The secretome was obtained by carefully aspirating the upper layer (1.5 mL) using a P1000 pipette, transferring it to a clean 15 mL Falcon tube, and centrifuging at 5000 rpm for 3 minutes to eliminate any residual cells or debris. The remaining volume in the well (500 µL), constituting the "ET fraction," was supplemented with 5U of DNase and 10X DNase buffer. After waiting for 40 min at 23°C, 400 µL from the upper layer were cautiously collected using a P200 pipette avoiding cell retrieval and transferred to a 2 mL Eppendorf tube. To halt the DNase reaction, 15 mM EDTA was added. Centrifugation of this fraction at 5000 rpm for 3 min eliminated any remaining cells or cellular debris, and the supernatant was transferred to a clean tube and frozen for subsequent mass spectrometry analysis. The remaining “Cell fraction” in the plate was collected and used for other analyses.

Before mass spectrometry analysis this protocol was tested by loading the “ET fraction” on an SDS page using silver staining to be able to visualize the proteome.

2.5.2 Mass Spectrometry Analysis

Sample preparation for mass spectrometry analysis and protein identification was done by Melisa Institute. The methods used were as follows:

2.5.2.1 Sample Preparation for MS

Samples were concentrated by lyophilization. Proteins were then extracted using chloroform/methanol, followed by equilibration, centrifugation, and washing with cold 80% acetone. The resulting protein pellet was air-dried. Samples were then resuspended in 30 µL of 8M urea and 25 mM ammonium bicarbonate. Reduction with DTT, alkylation with iodoacetamide, and dilution with ammonium bicarbonate followed.

2.5.2.2 Tryptic Digestion and Cleanup

Tryptic digestion was performed with a 1:50 protease-to-protein ratio. The reaction was stopped with 10% formic acid. Cleaned peptides were obtained using Sep-Pak C18 Spin Columns (Waters) and then dried in a rotary concentrator.

2.5.2.3 LC-MS/MS Analysis

200 ng of peptides were injected into a nanoUHPLC nanoElute coupled with a timsTOF Pro mass spectrometer (Bruker Daltonics). Liquid chromatography utilized a 90-min gradient of 2% to 35% buffer B (0.1% formic acid – acetonitrile). Data collection employed TimsControl 2.0 with 10 PASEF cycles, mass range of 100-1700 m/z, and specified instrument settings.

2.5.2.4 Protein Identification

MSFragger version 3.5 (Kong et al., 2017) through the Fragpipe version 18.0 platform was used for data analysis with parameters such as precursor mass tolerance, fragment mass tolerance, and enzymatic digestion specificity. Carbamidomethylation was set as a fixed

modification, while oxidation of methionine, N-terminal acetylation, and deamination of asparagine and glutamine were considered variable. Identification utilized the *D. discoideum* standard proteome from Uniprot with FDR estimation, an FDR ≥ 1% filter and at least 1 unique peptide per protein. The resulting output consisted of tables containing data from three replicates for the ET fraction and the secretome, under control and induction conditions by LPS from *K. pneumoniae*.

2.5.3 Bioinformatic Analysis

A comprehensive bioinformatic pipeline was implemented using R programming language and various specialized packages in the proteomic analysis conducted. The initial steps involved reading and processing protein abundance data from the two experimental conditions from both the ET fraction and the secretome (Figure 3). All the proteins found were then mapped against a database containing all mitochondrial proteins of *D. discoideum* (Freitas et al., 2022). Filtering was performed to select proteins expressed in at least two replicates and with intensities greater than zero. Subsequently, spectral count filtering was applied, and proteins with total spectral counts below 3 were excluded. The filtered proteins were then mapped against the PANTHER *D. discoideum* Protein Class database (Thomas et al., 2022). Also, the proportion of unknown filtered proteins was determined in both conditions using a simple filter based on UniProt annotation (Bateman et al., 2023). The filtered dataset underwent normalization by log2 transformation and median-centering for each replicate to calculate log-fold changes between conditions. Statistical significance was determined using a two-sample t-test, and p-values were adjusted for multiple testing using the Benjamini-Hochberg method (Benjaminit & Hochberg, 1995)The analysis was facilitated by R packages such as tidyverse (Wickham et al., 2019), ggVennDiagram (Gao et al., 2021)

and ComplexHeatmap (Gu et al., 2016), each contributing to distinct aspects of data manipulation, visualization, and statistical testing. Finally, Foldseek was utilized to identify a human structural homolog for one of the proteins differentially expressed under control conditions (van Kempen et al., 2023). The query protein structure from *D. discoideum* was determined using Alphafold (Jumper et al., 2021).

3 RESULTS

3.1 Extracellular Trap release kinetics upon LPS stimulation

We set up a fluorescence-based microplate reader assay to ascertain the optimal conditions for inducing ETosis in vegetative *D. discoideum* cells. Utilizing a widely used DNA-binding fluorescent probe that predominantly remains in the extracellular space, Sytox Green, we monitored fluorescence as an indicator of secreted DNA and, consequently, ETs production. Drawing upon what tested for ETs produced by *D. discoideum* S cells, we initiated our investigations with 5 µg/mL LPS from *K. pneumoniae*. Subsequently, we explored variations, testing concentrations at half and double the initial dosage, along with LPS from *S. enterica*. Our preliminary observations revealed that fluorescence levels reached a plateau approximately 4 h post-induction (Figure 4). Notably, based on prior results from our group involving microscopy and flow cytometry experiments, we acknowledged the potential impact of physiological changes induced by starvation on cell size and membrane permeability. This insight may explain the increased Sytox Green fluorescence signal in the control after approximately 6 h (Figure 4). To mitigate the risk of prolonged incubation influencing data integrity and experiment feasibility, we established 4 h post-induction as a

reference point for studying ET production in vegetative *D. discoideum* cells. Subsequent analyses were consistently conducted at this time point to ensure robust and reliable results.

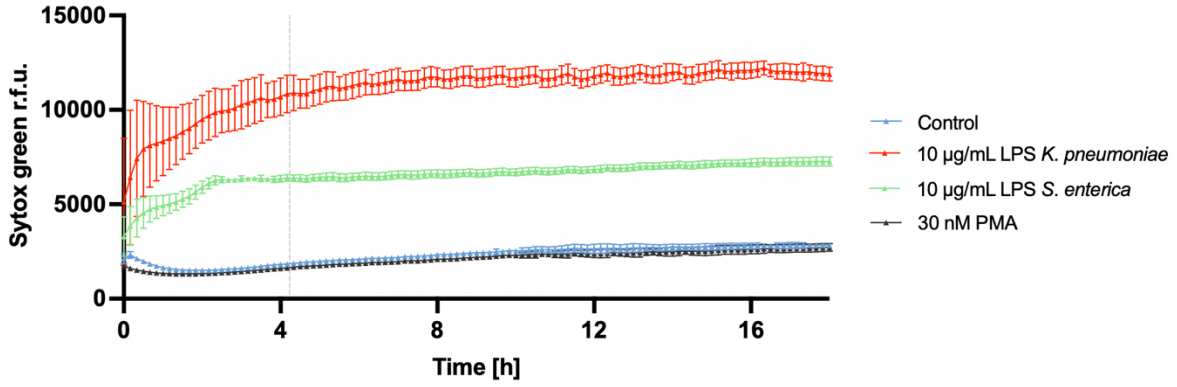

Figure 4. Sytox Green Fluorescence Over Time Induced by LPS and PMA for 18 Hours. The grey bar at the 4-hour mark signifies the specific time point chosen for conducting all experiments, providing a reference point for the subsequent analyses.

The dosage-dependent behavior of the observed phenomenon is evident (Figure 5). A notable increase in fluorescent signal is observed after 4 h of induction, particularly with the highest concentration of LPS from *K. pneumoniae* used, in stark contrast to the control. A more modest effect is discerned when utilizing half of the concentration of LPS from *K. pneumoniae* (5 µg/mL), with significance comparable to the use of 10 µg/mL of LPS from *S. enterica*. Conversely, no statistically significant differences are noted with the application of lower concentrations of LPS from *S. enterica* or the minimum concentration of LPS from *K. pneumoniae*.

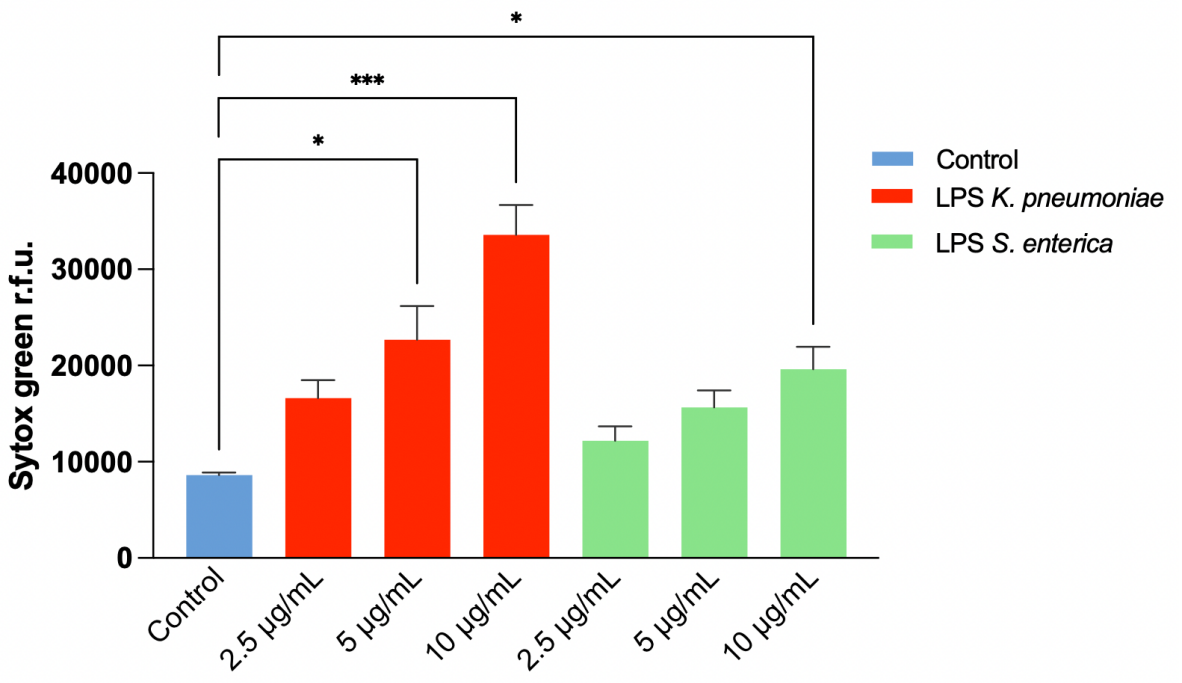

Figure 5. Extracellular Trap Release Dependency on LPS Concentration. Vegetative cells were seeded in a 96-well plate with a DNA probe (Sytox Green) and measured using a Tecan microplate reader. The statistical analysis was conducted using multiple comparisons ANOVA (Friedman test) (* $p < 0.05$, ** $p < 0.01$, *** $p < 0.001$).

To confirm that the observed increase in fluorescence specifically resulted from extracellular traps (ETs) rather than cell death, we visually examined the cells. Cells were stimulated with the same concentrations of LPS, and Sytox Green fluorescence was measured under the conditions previously mentioned in the microplate reader. After 4 hours of measurements, the same plate was visualized under an automated fluorescence microscope (Figure 6). This analysis revealed the same dosage-dependent behavior as observed in the microplate reader. Despite a slight leakage of Sytox Green into the nucleus, even in the control condition, cells across all conditions maintained a rounded shape similar to the control. This observation suggests that the measured fluorescence primarily originates from secreted DNA, and the majority of cells remain viable.

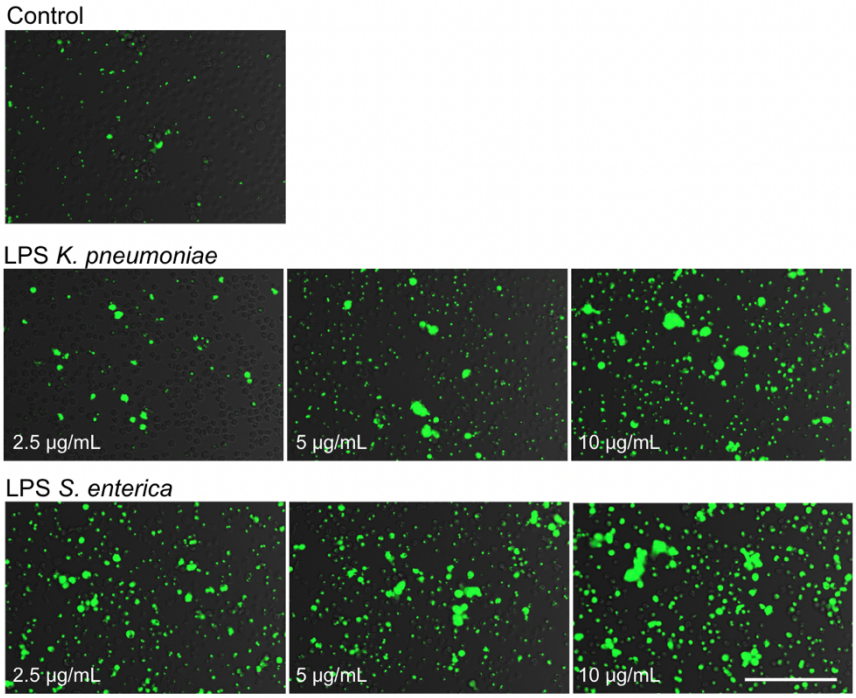

Figure 6. Sytox Green Fluorescence in Cells Induced by LPS and Visualized in an Automated Fluorescence Microscope. Representative images of the different conditions were captured after 4 hours of induction previously measured in a microplate reader. Scale bar: 100 µm

The experimental procedures throughout this thesis were conducted using the AX2 strain instead of the AX4 strain, which is conventionally utilized in our lab for host-pathogen interaction experiments. Although AX4 and AX2 exhibit broad similarities, genetic and behavioral distinctions have been noted (Bloomfield et al., 2008). The AX2 strain is particularly favored in *D. discoideum* research on a global scale, owing to its extensive use and the availability of more mutants than the AX4 strain. Despite these disparities, we found it pertinent to explore ETs in AX4 as well briefly.

Consequently, we expanded our investigation to include AX4 strains, employing the highest concentrations of both LPS tested in AX2 alongside varying concentrations of PMA—a well-established extracellular trap inducer (Figure 7). The impact of LPS in AX4

closely mirrored what was observed in AX2. Conversely, PMA demonstrated minimal effect on cells in both AX2 and AX4 across different concentrations and also showed a detrimental effect on cells, pointing out a notable difference with the potent NET-inducing effect observed in neutrophils (Supplementary Figure 1).

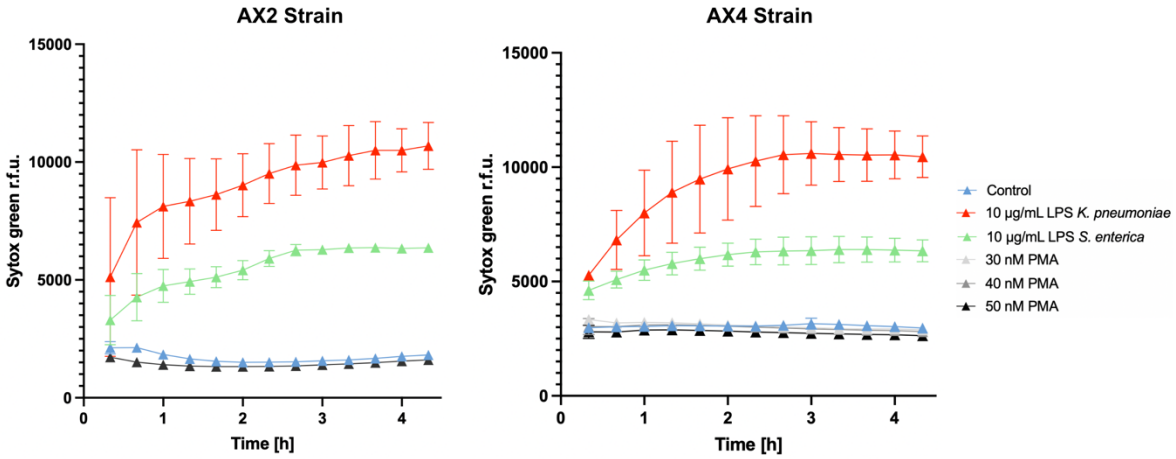

Figure 7. ETs Over Time Induced by LPS and PMA in AX2 and AX4 Strains. Vegetative cells were seeded in a 96-well plate with a DNA probe (Sytox Green) and measured using a Tecan microplate reader at 20-min intervals. The experiment involved the induction with both LPS and PMA, with different concentrations of PMA. Data is presented for both AX2 and AX4 strains.

3.2 Extracellular Trap visualization by automated fluorescence microscopy

Once the appropriate concentration and timing were determined, we visualized ETs in more detail. A comprehensive review of the literature highlighted the variability in the appearance of ETs, influenced by multiple factors. Nevertheless, we used the observations in S cells as a reference for visualizing ETs. We first look at them in strains AX4 and AX2 for a more general view of cells induced only by LPS from *K. pneumoniae.* Interestingly, as seen in S cells, aggregates form in both strains (Figure 8).

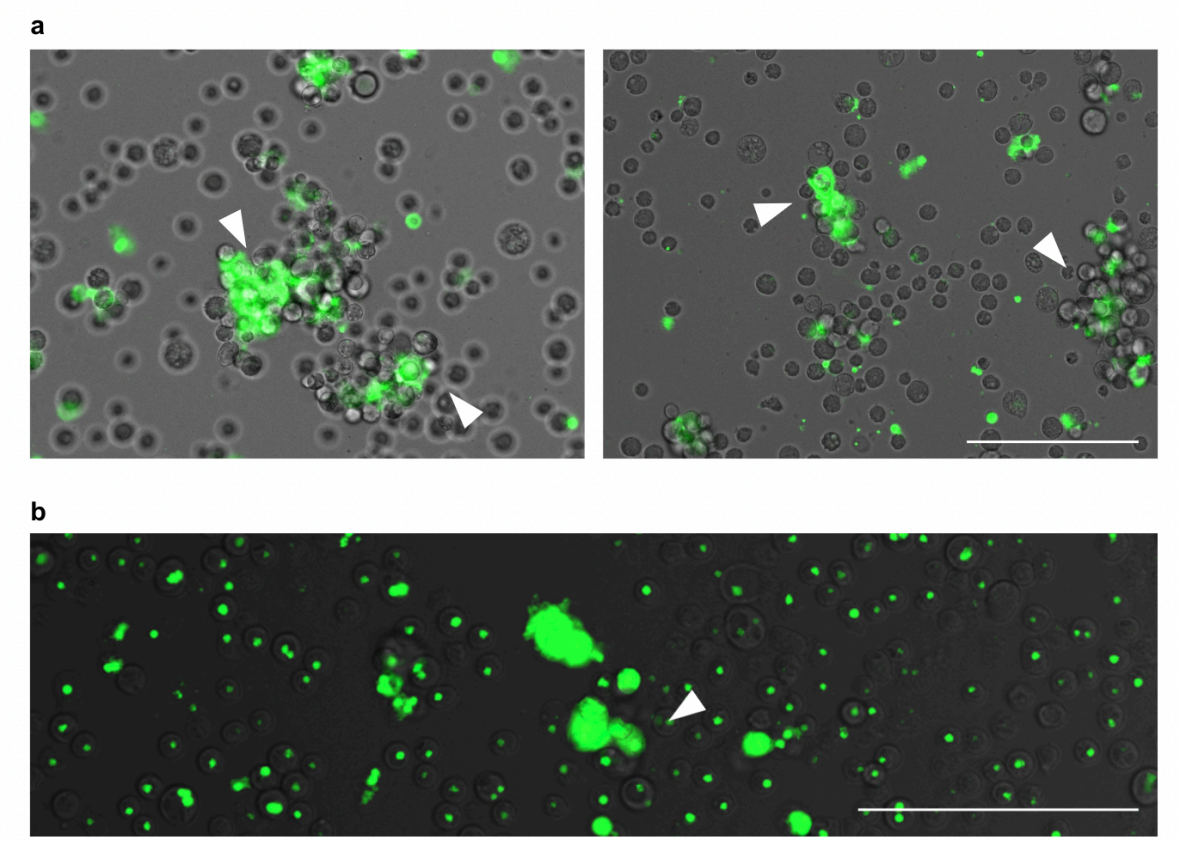

Figure 8. Representative Images of ETs forming ETs aggregates. Cells were visualized after 4 h of induction with LPS from *K. pneumoniae* from different strains: a) AX4 cells and b) AX2 cells. ET aggregates are highlighted by arrowheads and visualized clearly in the GFP channel using the Sytox Green probe. Scale bar: a) b) 100 µm.

Similarly, we visualized ETs induced by both LPS from *K. pneumoniae* and *S. enterica* in cells of the AX2 strain, showing the typical spiky-like appearance (Figure 9). It is important to note that the visualization of ETs was consistently more prevalent in response to LPS from *K. pneumoniae* stimulation. Apparently, more cells are actively producing ETs upon LPS from *K. pneumoniae*. This trend is further evident when observing a larger area of the well where multiple cells are present (Supplementary Figure 2).

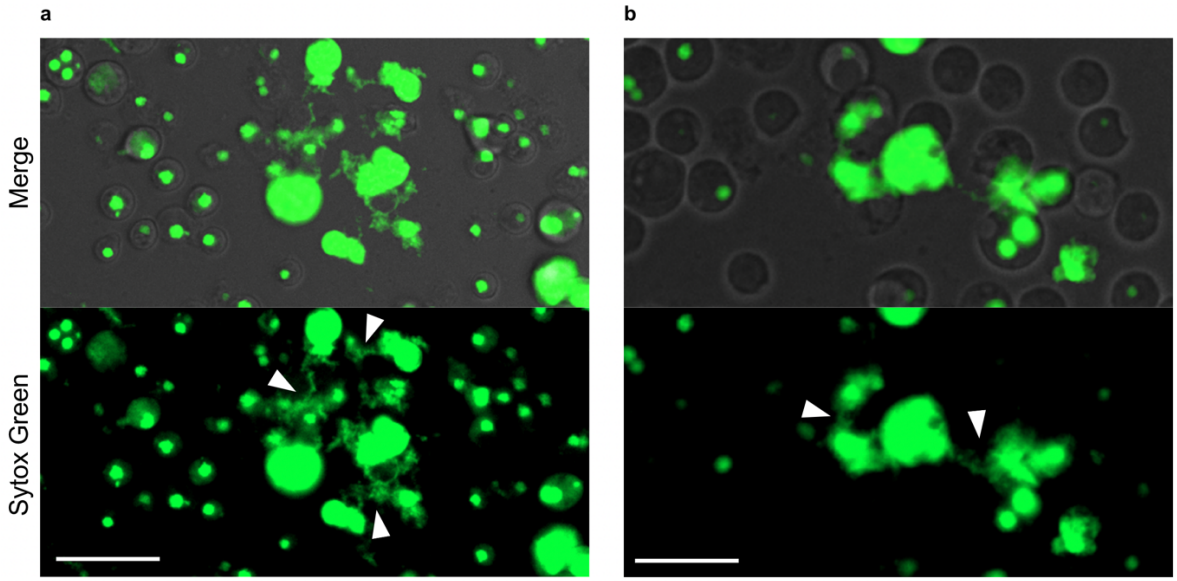

Figure 9. Representative Images of ETs Induced by LPS from *K. pneumoniae* and *S. enterica*. Cells were visualized in a 96-well plate after 4 h of induction with a) LPS from *K. pneumoniae* and b) LPS from *S. enterica*. Extracellular traps (arrowheads) were visualized in the GFP channel using the Sytox Green probe. Scale bar: 30 µm (left); 20 µm (right).

We recorded a substantial portion of a well to capture the dynamic process of a single cell undergoing ETosis, allowing us to visualize one of these events. Approximately 150 to 200 cells were observed simultaneously (Supplementary Figure 2). Although the process initiates within a few minutes, as indicated by the microplate reader (Figure 7), the live capture of ET

formation occurred slightly later (Figure 10). Consequently, while some cells may initiate the process rapidly, it continues to unfold over time, with more cells engaging in the ET formation process.

The observation sequence typically begins with an intact cell displaying no Sytox fluorescence and maintaining its original shape. Shortly after that, a change is observed in one part of the cell membrane, possibly a rupture, followed immediately by the appearance of Sytox fluorescence, indicating the release of DNA through that specific region. This phenomenon was captured during induction with both LPS from *K. pneumoniae* and *S. enterica* (Figure 10).

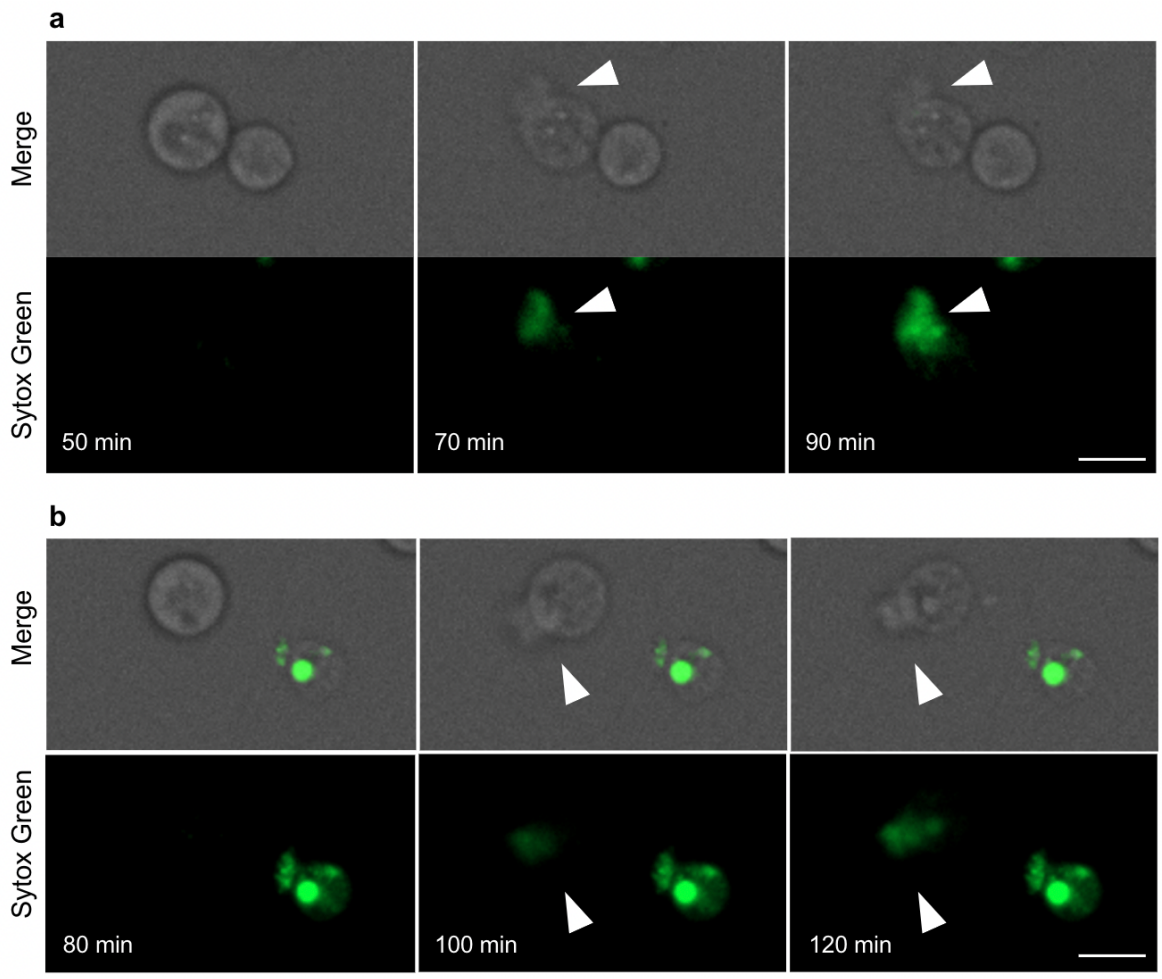

Figure 10. ETs Release Captured in a Single Cell. Extracellular trap release events were captured at the single cell level under two conditions: a) LPS from *K. pneumoniae* and b) LPS from *S. enterica*. Arrowheads indicate the release in both conditions, visualized in the GFP channel using the Sytox Green probe. Scale bar: 10 µm.

DNAse treatment was applied to elucidate the association between the identified Sytox fluorescence and the DNA release corresponding to the production of ETs. Sequential images of cells stimulated with LPS for 4 h were captured before and after DNAse treatment at identical positions (Figure 11). These images reveal that DNA demarcated just outside the cell and in direct contact with it undergoes a discernible loss of Sytox fluorescence post-treatment. This reduction in fluorescence serves as an indicator of the structural disruption

induced by the employed endonuclease. Notably, a residual fluorescence persists within the cell after treatment. This enduring fluorescence can be attributed to the prior infiltration of Sytox during the membrane disruption characteristic of ETosis. Consequently, the accumulated fluorescence within the nucleus persists even after DNAse treatment.

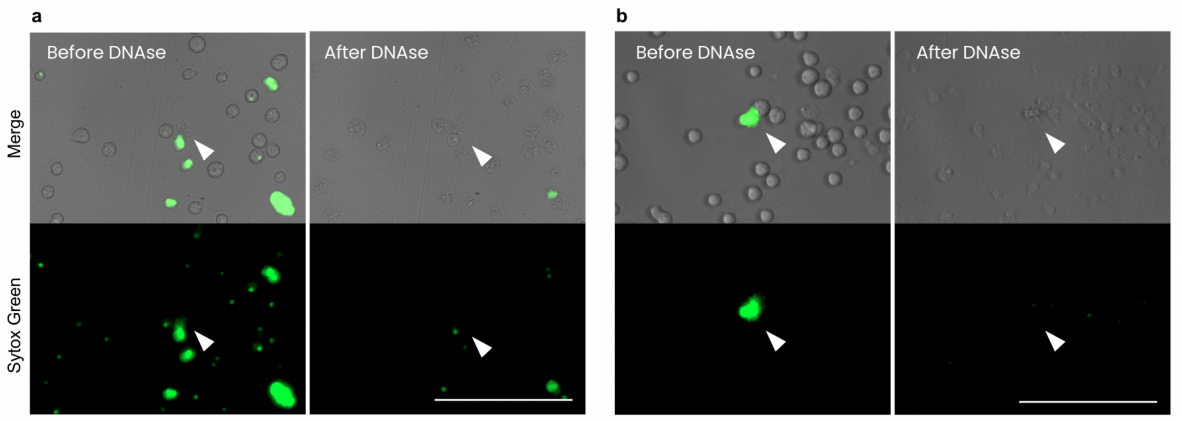

Figure 11. DNAse Treatment Effects on ETs. Extracellular traps induced by a) LPS from *K. pneumoniae*, and b) LPS from *S. enterica* were treated with DNAse. Arrowheads indicate the site of the extracellular trap before (left) and after (right) treatment. Scale bar: 100 µm.

3.4 Extracellular Traps DNA nature

As mentioned earlier, the origin of extracellular trap DNA can differ based on the cell type and the stimuli and conditions involved. To characterize the nature of secreted DNA, we employed an approach previously used for this purpose (Morshed et al., 2014; Zhang et al., 2016). Using specific primers targeting the mitochondrial gene *rnl* and the nuclear gene *h3a* (Supplementary Table 2), we conducted quantitative PCR (qPCR) to estimate the content of mitochondrial DNA (mtDNA) and nuclear DNA in the "ET fraction" -the fraction in closer proximity to the cells when removing the “secretome”- and the “Cell fraction” -the cells attached to the well- (Figure 3). Our objective was to determine the proportion of both types

of DNA in both fractions and explore potential differences when induced by *K. pneumoniae* or *S. enterica* LPS.

As illustrated in Figure 12, there is a noticeable increase of mtDNA in the "ET fraction" upon cellular stimulation with LPS from both bacterial strains. Notably, even without induction, the "ET fraction" still has mitochondrial and nuclear DNA. However, the proportional increase is marked, particularly in the amount of mtDNA. Additionally, it is worth highlighting the subtle distinctions between the stimulations with LPS from *K. pneumoniae* and *S. enterica* in the ET fraction, with the latter exhibiting a slightly lower amount of mtDNA secretion. Intriguingly, the DNA content of the "Cell fraction" remained unchanged, indicating no significant difference across all conditions. These results suggest a specific mtDNA enrichment in the "ET fraction" induced by the LPS stimuli not seen in the "cell fraction".

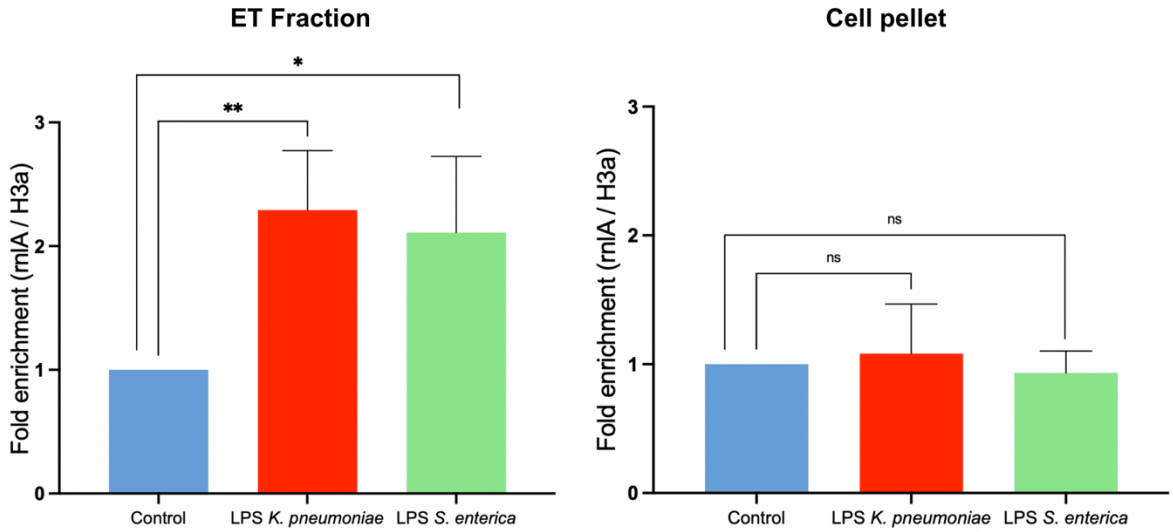

Figure 12. Enrichment of mtDNA in Extracellular Trap Fraction of Induced Cells. Induced by LPS from *K. pneumoniae* and *S. enterica*. A representative result from three independent experiments performed in triplicates is shown. Compared with the control, the range of relative folds of enrichment of mitochondrial DNA (*rnlA* gene) versus nuclear DNA (*H3a* gene) was calculated using the Pfaffl method. The non-induced condition was a

reference for the ET fraction and the cellular pellet. A two-sample unpaired t-test was performed to compare the control with the induced condition. (* $p < 0.05$, ** $p < 0.01$, *** $p < 0.001$).

3.3 Extracellular Traps Proteomic Analysis

Since the discovery of ETs in neutrophils, the association of proteins with these DNA structures has been well-established (Brinkmann, 2004). Recent research endeavors (Chapman et al., 2019; Petretto et al., 2019; Scieszka et al., 2022; Urban et al., 2009) have concentrated on elucidating the global proteomic profile of these structures. To comprehensively characterize ETs from vegetative cells of *D. discoideum*, we developed a protocol for extracting and mass spectrometry analysis of proteins associated with these structures.

In brief, the "ET fraction" and "secretome" underwent analysis, originating from cells initially seeded in Sorensen buffer and induced with LPS from *K. pneumoniae*, while control conditions received buffer alone. To liberate proteins from the DNA structure, the "ET fraction" underwent treatment with DNase. Subsequently, both the "ET fraction" and "secretome" were processed for mass spectrometry, involving protein extraction, digestion, and preparation for LC-MS/MS analysis. Identification of proteins utilized *Dictyostelium discoideum* proteome as a reference, with various bioinformatic tools applied for qualitative and quantitative analyses. By comparing proteins in the "ET fraction" with the ones in the whole secretome, we aimed to further validate the specificity of our protocol.

Upon comparing the “ET fraction” with the secretome under each condition, we identified proteins exclusive to each fraction. Intriguingly, more proteins were exclusively associated with the “ET fraction” in the induction by LPS *K. pneumoniae* compared to the control condition (Figure 13a). We also compared proteins found in both “ET fractions” using

an existing database of mitochondrial proteins of *D. discoideum* (Freitas et al., 2022). Out of the 936 proteins identified in this organism's mitochondria, 426 were found to be present in the "ET fraction" of the control and induced condition. Intriguingly, our analysis revealed the presence of seven proteins exclusively found in the condition induced by LPS from *K. pneumoniae* (Figure 13b), all of which have their human homologs.

To enhance the rigor of our analysis in comparing the ET fraction of the induced and control conditions, we applied stringent bioinformatics filters and criteria to filter the data. Specifically, a protein was considered present only if it was detected in at least two replicates and had a minimum of 3 spectral counts. Subsequently, comparing the filtered "ET fraction" under both conditions, we observed an 83% overlap in proteins alongside proteins exclusive to each condition (Figure 13c).

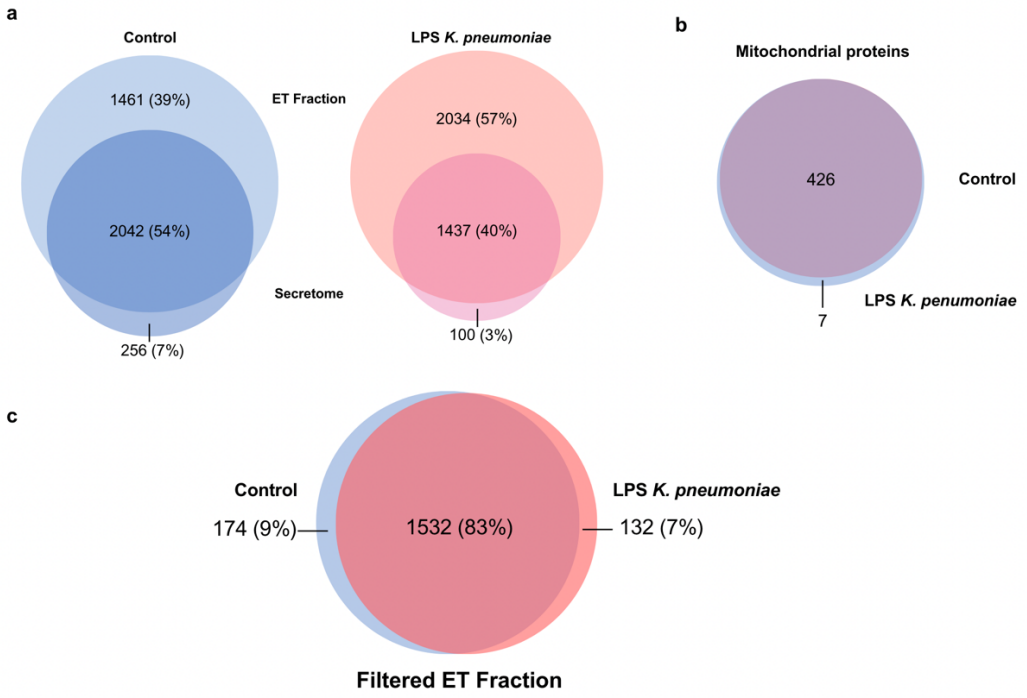

Figure 13. Venn Diagrams of proteins present on the ET fraction. Venn Diagrams of proteins present on the ET fraction of *D. discoideum* vegetative cells when induced by *K.*

pneumoniae LPS and control. a) Venn diagram of the ET fraction against the secretome fraction for the control and induced condition b) Mitochondrial proteins of the ET fraction in the control and induced condition c) Venn diagram of control and LPS from *K. pneumoniae* induced filtered ET fraction.

Subsequently, we focused on the functional analysis of the global proteomic profiles in both conditions (Figure 14). Leveraging the Panther database, we quantified the number of proteins associated with specific protein classes in both conditions. Notably, a substantial portion of proteins in the *D. discoideum* proteome lacked assignment to a specific protein class; hence, the "unclassified" category was excluded from the plot to enhance clarity regarding the quantities of each category. In general terms, a comparable number of proteins were detected for each category in both conditions. The most notable difference appeared in the 'transporter' class, revealing a reduced identification of proteins within this category under the induced condition.

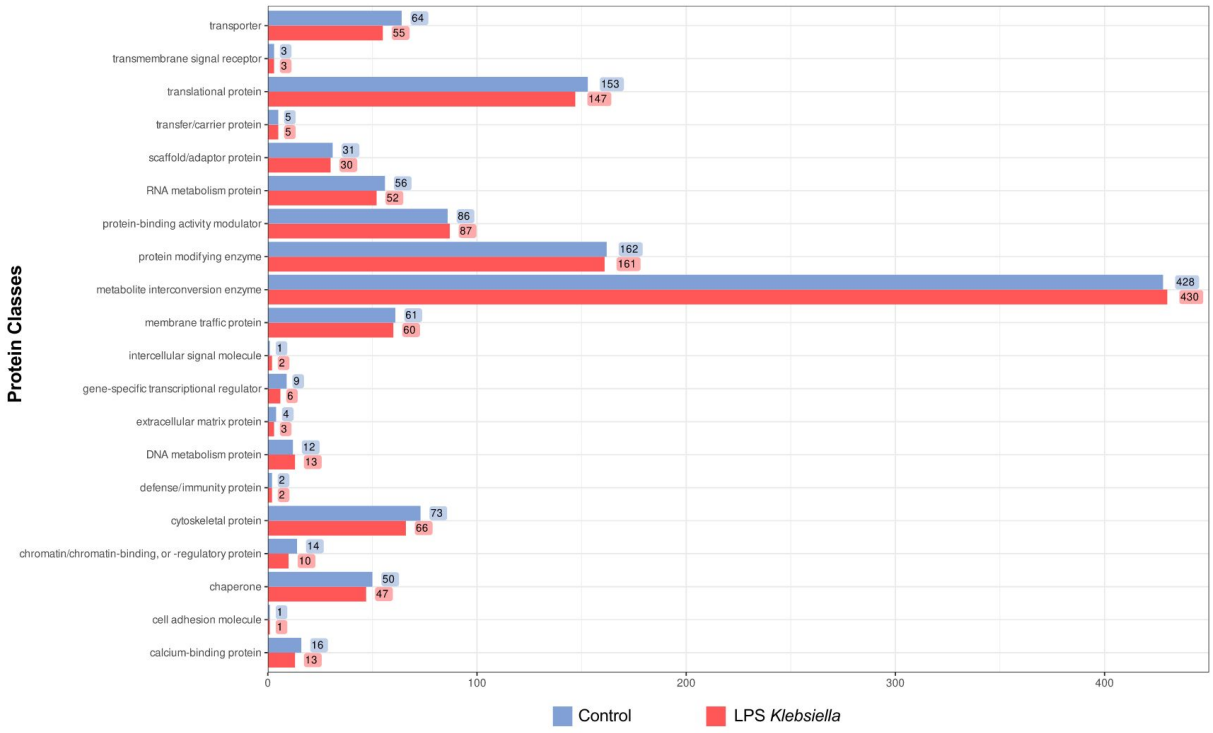

Figure 14. Comparative Analysis of Protein Abundance Across Different Protein Classes. Comparative Analysis of Control and Induced by LPS from *K. pneumoniae*. Each bar represents the number of proteins within a specific class, Control is denoted in blue whereas *K. pneumoniae* LPS-induced condition is in red.

Further scrutiny of the two conditions involved a quantitative approach, where we compared protein intensities and determined differentially expressed proteins. Total intensity served as a measure of the abundance of specific proteins, revealing both differentially expressed proteins in the induced and control conditions, as depicted in the volcano plot (Figure 15). Notably, most of the proteins differentially expressed in the induced condition were annotated as "unknown". Additionally, two proteins of the short-chain dehydrogenase/reductase family protein were also found to be enriched in this condition (DDB_G0283727 and DDB_G0272466).

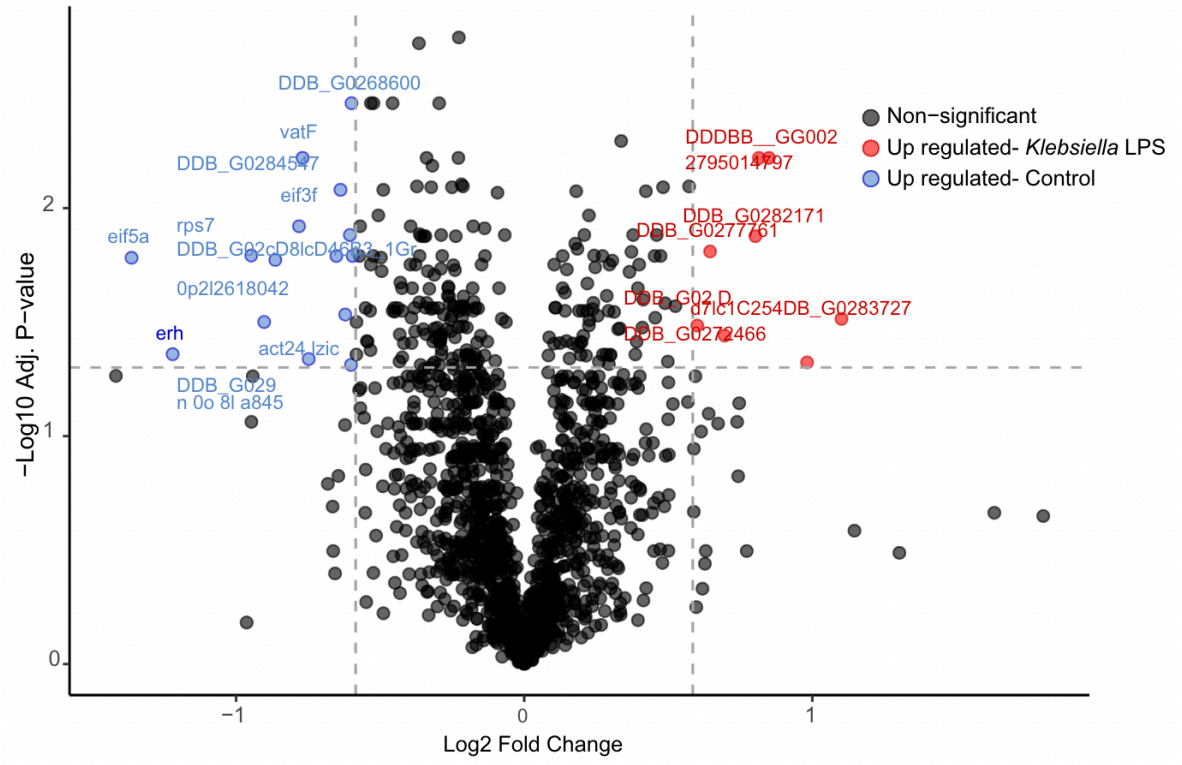

Figure 15. Volcano plot of differentially expressed protein. Black dots represent proteins with a Log2 fold-change smaller than 0.5 and a p-value inferior to 1.5, thus nonsignificant. Up-regulated proteins in the condition treated with *K. pneumoniae* LPS are in red, whereas blue dots represent up-regulated proteins in the control condition.

A detailed analysis of proteins with a significant fold change in both conditions, represented through a heatmap (Figure 16), revealed a diverse array of enriched protein classes in the control condition. In contrast, proteins enriched in the induced condition included predominantly metabolite interconversion enzymes (4), where the two proteins of the short-chain dehydrogenase/reductase family belong, followed by three with an unknown protein class and one cytoskeletal protein.

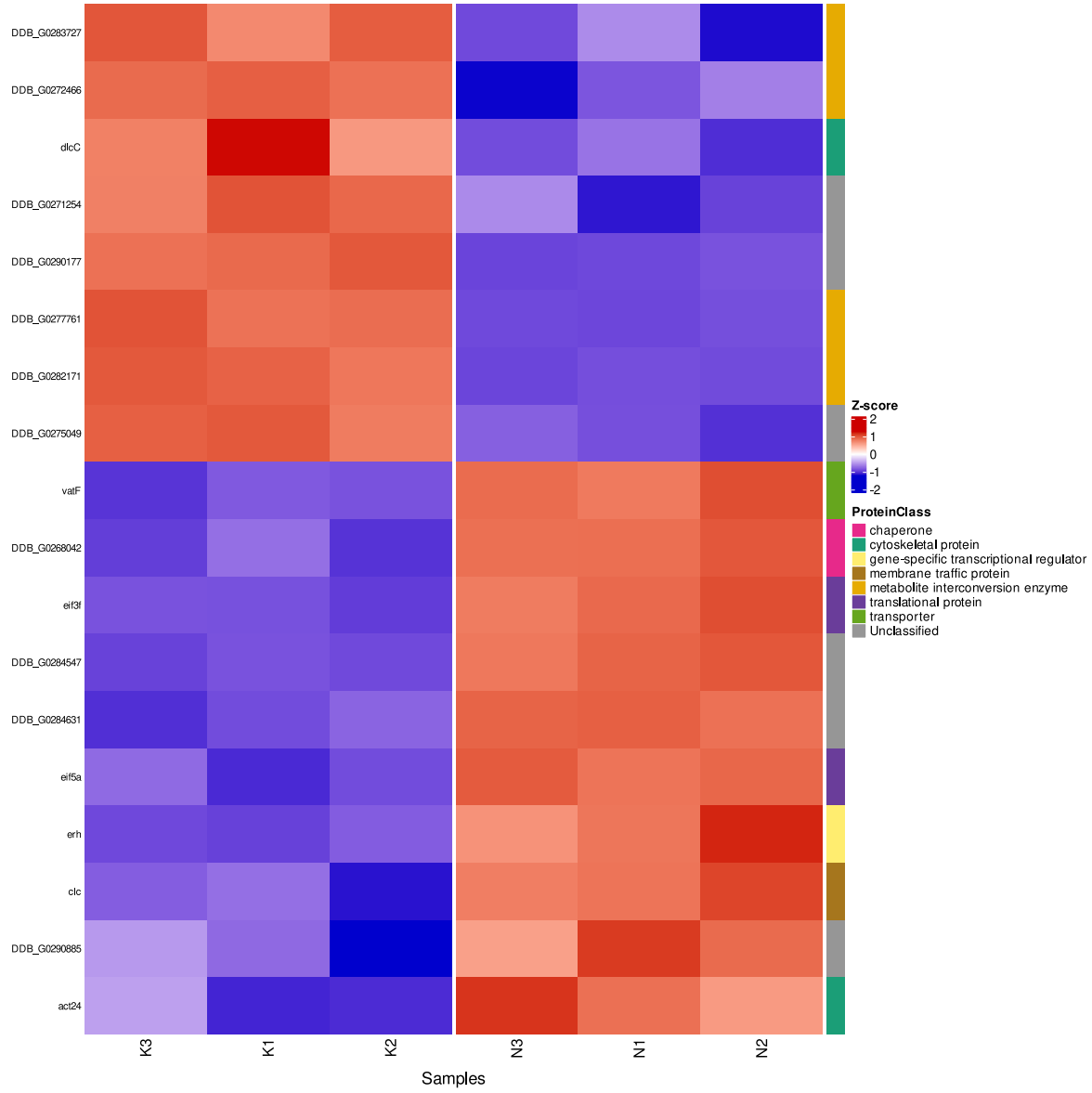

Figure 16. Heatmap of the proteomic profile of differentially expressed proteins. Heatmap representation of the proteomic profile of ET fraction of differentially expressed proteins in *D. discoideum* vegetive cells under control and induced condition with LPS from *K. pneumoniae.* The heatmap illustrates the differential expression patterns of proteins across two conditions, with rows representing individual proteins and columns corresponding to biological replicates. Colors indicate the normalized Z scores, visually depicting the intensity levels, where warmer colors signify more abundance and cooler colors signify less abundance. Protein classes are highlighted, offering insights into the functional diversity of the identified proteins.

Considering that a substantial number of proteins in *D. discoideum* are categorized as "unknown" in the database employed, we aimed to compare this fraction of the entire proteome with the proteome of each explored “ET fraction” (Figure 17a). We observed similarities in the total proportion of unknown proteins detected in both categories. However, a distinctive feature emerged as this fraction differed from the rest of the proteome, exhibiting a smaller proportion of unknown proteins. This finding is compelling evidence that our investigation targets a unique protein fraction rather than examining the entire cellular proteome.

Subsequently, considering the proportion of unknown proteins that were enriched during induction with LPS *K. pneumoniae*, and intending to establish a foundation for future investigations into this category of proteins, we conducted a structural alignment for one of the unknown proteins differentially expressed against the human proteome (Figure 17b). Specifically, we selected the DDB_G0284547 protein and employed Foldseek to identify its structural homolog in humans. The analysis revealed a compelling alignment with a human calcium-binding mitochondrial protein. This alignment, characterized by a Template Modeling (TM) score of 0.56, holds significant promise in elucidating the potential function of the previously unidentified protein. It also serves as compelling evidence to warrant further analysis and exploration of unknown proteins in the context of their structural and functional characteristics.

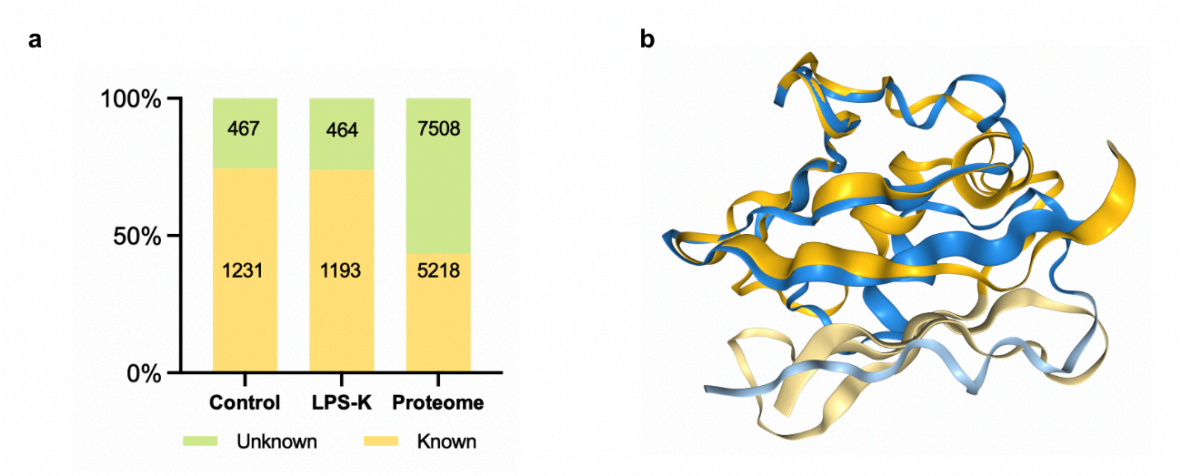

Figure 17. Unknown proteins in ET fraction of control and induced cells. A) Percentage of known and unknown filtered proteins in both conditions compared to the total *D. discoideum* proteome. B) Structural analysis of an unidentified *Dictyostelium* protein (depicted in blue) shown in alignment with its human structural homolog (depicted in yellow), as determined by Foldseek. Lighter colors represent regions that did not align, highlighting potential structural variations between the *Dictyostelium* and human homologs.

4 DISCUSSION

4.1 Extracellular Traps Induction

Various inducers have been identified to stimulate the formation of ETs across different cell types (Daniel et al., 2019; Goldmann & Medina, 2012). The efficacy of these is influenced by the concentration employed (Hoppenbrouwers et al., 2017). As mentioned, PMA, (Kenny et al., 2017) LPS, and bacteria (Goldmann & Medina, 2012), are widely used as ET inducers in neutrophils and other immune cells. The last two have also been used in *D. discoideum* S cells (Zhang et al., 2016).

In our quest to optimize conditions for inducing ETs in *D. discoideum* vegetative cells, our experiments focused on these various inducers, their concentrations, and the timing of induction. Using a microplate reader to measure a DNA binding fluorescence dye as a metric for ET release is a widely employed method (Carmona-Rivera & Kaplan, 2016; Chapman et al., 2019; Zhang et al., 2016). In our initial experiments, LPS from *K. pneumoniae* was employed at 5 µg/mL, guided by references on *D. discoideum* ETs in S cells. We explored variations, testing double and half concentrations of this LPS and LPS from *S. enterica*. Additionally, we investigated the common ET inducer, PMA, starting with a concentration near the smallest previously reported (Urban et al., 2009).

Dosage dependency of ETosis became evident, with the highest concentration of *K. pneumoniae* LPS inducing a notable increase in fluorescent signal after 4 h, compared to controls. Lower concentrations of LPS *K. pneumoniae*, as well as *S. enterica* LPS, exhibited more modest effects. Notably, no statistically significant differences were observed with

lower concentrations of LPS *S. enterica* or the minimum concentration of LPS *K. pneumoniae* (Figure 5). This result underscores the common dosage-dependent nature of ET induction when testing different activators (Scieszka et al., 2022).

To investigate the impact of the classical ETosis inducer, different concentrations of PMA were tested, revealing minimal effectiveness in eliciting ETosis in both strains of *D. discoideum.* The baseline fluorescence of PMA-induced cells remained consistent over time, resembling the non-stimulated condition, indicating a lack of significant response to PMA stimulation. Furthermore, a detrimental effect on cells was observed across the concentrations employed (figure S1). To interpret these findings, it is crucial to consider the established effects of PMA on neutrophils and other immune cells. PMA functions by mimicking the action of diacylglycerol (DAG), thereby activating PKC and subsequently triggering ETosis (Damascena et al., 2022), as previously mentioned. Although it is plausible that DAG-regulated kinases may exist in *D. discoideum*, the absence of PKC in this organism (Goldberg et al., 2006) suggests the involvement of an alternative mechanism in ETosis induction, which warrants further elucidation.

Regarding the kinetics of this process, a consistent elevation in fluorescence levels during LPS induction was observed in both AX2 and AX4 strains at each 20-minute interval (Figure 7), indicating that ET release occurs within this timeframe. This observation is supported by our microscopy findings (Figure 10). Additionally, our microplate reader measurements were initiated approximately 15 min after actual induction and revealed higher initial Sytox fluorescence readings in LPS-induced samples compared to the control. Similar observations have been noted in S cells, where a rapid surge in fluorescence within minutes was documented (Zhang et al., 2016). Early neutrophil investigations underscore that the process can initiate as early as 10 min after activation (Brinkmann et al., 2004).

Subsequent studies have identified an even swifter non-lytic NETosis mechanism evident both *in vitro* and *in vivo* (Pilsczek et al., 2010; Yipp et al., 2012). An even faster ETosis mechanism has been reported in eosinophils, requiring seconds to release mtDNA (Yousefi et al., 2008). Our observations seamlessly align with an ETosis process. Once technical difficulties are overcome, faster recordings should be conducted in vegetative *D. discoideum* cells to detail the process further. This is especially pertinent considering our qPCR data indicating mitochondrial DNA secretion, suggesting a potential mechanism akin to vital mtDNA ETosis.

Concerning the temporal aspect, our observations revealed that, under LPS induction, fluorescence levels in AX2 strain stabilized at a plateau around 4 h post-induction (Figure 4). This specific 4 h timeframe aligns with established practices in investigating ETosis in neutrophils (Urban et al., 2009) and was similarly applied in examining ETs in S cells (Zhang et al., 2016). The adoption of this particular time point as a reference for studying ETs was substantiated by our current findings and the previously documented changes in *D. discoideum* cells upon more extended periods of observation.

In conclusion, our results aimed to optimize conditions for inducing ETs in *D. discoideum* vegetative cells, exploring various inducers, including PMA and LPS. The observed dosage dependency aligns with previous findings in ET induction, while the kinetic and timing of the process are consistent with studies of ETosis in other cell types. Interestingly, PMA demonstrated minimal effects and even proved detrimental to cells. These insights refine our understanding of ETosis in vegetative cells and emphasize the importance of meticulous experimental design to unravel cell-type-specific responses to inducers.

4.2 Extracellular traps appearance

When first identified in neutrophils, ETs were initially portrayed as external fibers comprised of nuclear and granule components (Brinkmann et al., 2004). Subsequent investigations then uncovered the variability in the appearance of ETs, influenced by various factors such as cell type, inductor, and even cell concentration (Daniel et al., 2019). Our initial objective was to characterize the appearance of these traps once the induction conditions were established.

Building on observations from S cells as a reference, we investigated the release of ETs in both AX4 and AX2 strains induced by LPS from *K. pneumoniae*. The resulting images show the formation of ETs aggregates (Figure 8), resembling those observed in S cells and in prior experiments within our group where ETs were induced by different bacterial strains (Farías-Moreno & Chavez Espinosa, 2021). Classical spiky-like structures reported in S cells and immune cells were also identified; however, it is noteworthy to emphasize this distinctive aggregation structure.

Despite aggregation being inherent to the life cycle of *D. discoideum* (Dormann et al., 2002), its occurrence in this instance is notably early and involves smaller structures. Consequently, what is observed does not result from starvation-induced commitment to multicellularity. This intriguing observation leads us to hypothesize that the stimulation triggering ETs production may play a role in facilitating cell attachment. Moreover, there is a possibility that a combination of non-ETosis and ET-producer cells contributes to the formation of this aggregation structure, akin to observations in neutrophils.

Importantly, these findings parallel similar structures documented in neutrophils and immune cells of earthworms and crabs (Homa et al., 2016; Robb et al., 2014; Schauer et al., 2014). This underscores the conserved nature of such structures and the potential effects of ETs in cellular interactions that warrant further investigation.

Upon examination of the AX2 strain, our analysis delves into the successful visualization of ETs induced by LPS from *K. pneumoniae* and *S. enterica,* which closely resemble those observed in S cells (Figure 9). Intriguingly, a more pronounced prevalence of ET events emerges in response to LPS from *K. pneumoniae* stimulation. Live recording of ET formation in a cell population reveals a sustained and broader commitment to ETosis over time during induction with LPS from *K. pneumoniae*, compared to LPS from *S. enterica* (Figure 6, Supplementary Figure 2). This trend is further substantiated by microplate reader assays, where induction with LPS from *S. enterica* reaches a plateau of DNA secretion faster than induction with LPS from *K. pneumoniae* does (Figure 4).

However, ETs-producing cells should be individually counted over time to compare both conditions properly. Unfortunately, counting ETs poses a challenging task due to potential biases introduced by observers (Henneck et al., 2023), and even using algorithms is difficult, given the distinctive appearance of ETs. To address this challenge, alternative approaches, such as flow cytometry, must be considered to provide unbiased insights into the proportion of the cell population undergoing ETosis (Carmona-Rivera & Kaplan, 2016; Gavillet et al., 2015). This method facilitates quantification and enables comparisons of the proportion of cells committed to ETosis under different stimuli.

Nonetheless, *D. discoideum* has been observed to behave differently in response to various bacteria (Nasser et al., 2013), and variability in neutrophil ET production has been noted depending on the specific LPS used (Pieterse et al., 2016). Additionally, it has been seen that differences in the lipid A of LPS can module different immune responses (Steimle et al., 2016). Hence, it is conceivable that different receptors or pathways recognize different LPS and subsequent ET production in these cells, which could account for the observed

discrepancies in both LPS inductions. This adds a layer of complexity to our understanding of the intricate mechanisms underlying ET formation that require further exploration.

In examining a single cell undergoing ETosis, we discern a sequential process that initiates with what appears to be a membrane rupture, ultimately culminating in the release of DNA detected by Sytox fluorescence (Figure 10). Notably, the general aspect and timing of this event closely parallel those recorded in neutrophils and S cells upon induction by LPS. However, due to the resolution limitations of our analysis, additional observations cannot be acknowledged, such as the possibility of an event like eosinophils that occurs within seconds. Advanced single-cell microscopy technologies should be employed to further characterize ETosis, explore potential variations between different inducers, and assess its parallelism with other cell types.

In assessing ETosis through DNAse treatment, the resulting images post-treatment reveal a discernible loss of Sytox fluorescence outside the cell, indicative of structural disruption induced by DNAse (Figure 11). This method for confirming ETosis has been widely employed (Brinkmann et al., 2004; Robb et al., 2014; Zhang et al., 2016), with protocols across studies showing remarkable similarities. However, a key distinction lies in the temperature conditions. Unlike neutrophils and other immune cells that typically undergo ETosis at 37°C, the observed process occurs at a lower temperature (23°C). Utilizing Turbo DNAse under these conditions enhances efficiency and ensures reliable results at similar times, validating the effectiveness of DNAse treatment.

In conclusion, our examination of ETs visualization in *D. discoideum*, focusing on ETs induced by LPS from *K. pneumoniae* and *S. enterica* in the AX2 strain, reveals variations in the ET response to different stimuli. Despite this variability, our observations align with essential aspects of ETosis seen in mammalian and invertebrate immune cells, encompassing

the classical spiky-like aspect of ETs, the sequential process of DNA release, and the formation of aggregate structures. These findings lay the groundwork for further exploration into the dynamics and mechanisms of ETosis in *D. discoideum* vegetative cells, with a particular focus on single-cell microscopy analysis and complementary cell population analysis.

4.3 Extracellular Traps DNA nature

The exact mechanism of ETosis remains a subject of ongoing debate, with current understanding suggesting that DNA can originate from various cellular sources, including the nucleus, mitochondria, or even both (Goldmann & Medina, 2012). Thus, we explored the nature of ET DNA in *D. discoideum* vegetative cells. Our investigation specifically targeted ETs induced by LPS from *K. pneumoniae* and *S. enterica* in the AX2 strain.

We employed qPCR as our primary tool to dissect the composition of the secreted material. We aimed to amplify the "ET fraction" (Figure 3) and discern potential differences induced by the distinct stimuli by utilizing specific primers targeting mitochondrial and nuclear DNA.

The qPCR analysis revealed a significant increase in mitochondrial material within the "ET fraction" when cells were stimulated by LPS from *K. pneumoniae* and *S. enterica*. Interestingly, the cell pellet fraction remained relatively stable, emphasizing a distinct enrichment in the "ET fraction" induced by the stimuli. Despite this, only minor differences were discerned between the effects of LPS from *K. pneumoniae* and *S. enterica*. Notably,

these subtle distinctions may imply variations in the extent of cells engaging in ETosis, as discerned through microscopy and microplate reader analysis.

Furthermore, in the absence of induction, the “ET fraction” exhibited the presence of mitochondrial and nuclear DNA, albeit in smaller amounts. This raises the possibility that a small number of ETs may be produced even without stimuli, reminiscent of the spontaneous ETs observed in neutrophils (Kamoshida et al., 2017). The potential occurrence of non-stimulated ETs could be associated with the reported increase in ROS concentration during starvation in *D. discoideum* (Rafia & Saran, 2019). However, the narrow 4 h recording window and induction timing might not be sufficient to reach these higher concentrations. Additionally, it is plausible that the detected DNA represents a fraction of dead cells, contributing their material to the “ET fraction”. This aligns with the minimal changes in Sytox fluorescence observed in microplate reader analysis and microscopy.

The origin of DNA in cells undergoing this process has been explored across different cell types. Notably, ETs of *D. discoideum* S cells were predominantly identified as mitochondrial (Zhang et al., 2016), a finding that aligns with our observations in vegetative cells during this study. This intriguing discovery challenges the conventional notion of the suicidal nature of ETosis, as the released DNA is dispensable, and cells remain alive. This raises questions about the evolutionary aspects of this process, suggesting that its altruistic nature may have originated in organisms such as *D. discoideum*, where the sacrifice is minimal, and then intensified in more advanced organisms, exemplified by the suicidal behavior observed in mammalian neutrophils.

Our results have unveiled a noteworthy increase in mtDNA within the “ET fraction”. However, these findings predominantly illuminate the outcome of ETosis, prompting further investigation into the precise underlying mechanism. The integration of mutant strains and

the analysis of induced cell pellets will significantly contribute to a more profound comprehension of the proteins involved in this process (X. Wang et al., 2018). Additionally, employing mitochondrial binding fluorescent probes holds promise in shedding light on how this DNA is extruded – whether through vesicles or the previously observed catapult-like mechanism. These approaches collectively aim to unravel the intricate details of the molecular events underpinning ETosis in *D. discoideum* vegetative cells.

4.4 Extracellular Traps Proteomic profile

The investigation of proteins associated with ETs has evolved since their initial discovery, with early research primarily focusing on specific proteins related to neutrophil granules (Brinkmann et al., 2004). Recent endeavors have shifted towards a broader examination of the global proteomic profile of these structures. Notably, a proposed characteristic core protein profile, termed the "NETome," has been suggested, emphasizing the need for a comprehensive understanding of the proteomic profile of these structures (Scieszka et al., 2022).

Some aspects must be considered to investigate the proteomic profile of ETs comprehensively. Whether proteins are physically attached to the DNA or merely secreted, constituting part of the ETosis response, remains debatable. None of the protocols mentioned in the literature confirm the purity of proteins directly attached to the ETs; instead, they indicate an enrichment due to endonuclease treatment that liberates the proteins associated with the ETs. Thus, it is essential to recognize that these protocols also account for proteins that are not physically attached to the DNA but are still integral components of the broader ETosis proteome.

Diverse research groups exploring this phenomenon have adopted varying methodologies. Some exclusively utilized the secretome fraction, employing an endonuclease, while others processed the cell fraction with the same enzyme (Supplementary Table 1). It is noteworthy that these methodologies have predominantly been applied in neutrophils. Given the absence of precedent for such global proteomic analyses in *D. discoideum*, developing a specific protocol became imperative.

We initially attempted to employ protocols analogous to those used in neutrophils. Despite similarities in phagocytic capacities, pinocytosis, and chemotactic behavior, these two cell types have significant experimental differences. Notably, *D. discoideum* attachment to plates differs from that observed in neutrophils, rendering washing steps detrimental to the study of extracellular structures. Furthermore, a critical distinction arises in analyzing proteins associated with ETs from neutrophils: the DNA originates mainly from the nucleus, resulting in more considerable material and a greater surface area for protein association than the potential mtDNA secreted by *D. discoideum* cells. Correspondingly, in neutrophils and considering the most described mechanism of NETosis, nuclear DNA is merged in the cytosol with granules and other cytosolic content before being extruded outside. In contrast, if the DNA in *D. discoideum* originates from the mitochondria, we would anticipate fewer and a different array of associated proteins given the possible mechanisms of ET extrusion in this case (Conceição-Silva 2021).

From a methodological standpoint, our approach meticulously preserves the integrity of the cell fraction throughout the entire process, ensuring that most cells remain firmly attached to the bottom of the plate. The subsequent centrifugation step further guarantees the absence of cell or cell debris in the obtained fraction. The comprehensive nature of our study

is enhanced by the inclusion of the secretome fraction, enabling a detailed differentiation between the "ET fraction" and the "secretome." This comparative analysis proves pivotal in unraveling the distinct protein composition associated with extracellular traps and secreted proteins. Remarkably, our results unveil a substantial overlap in the protein composition between the “ET fraction” and the secretome. However, our findings also highlight more proteins uniquely associated with the “ET fraction”, particularly in the induced condition compared to the control (Figure 13a). This observation suggests a specific and potentially heightened response regarding protein association with ETs under the influence of LPS from *K. pneumoniae* induction, emphasizing the dynamic nature of these structures in different cellular conditions.

In the analysis of results, notable differences emerge between the unstimulated condition and the *K. pneumoniae* LPS-induced condition. The enrichment of unknown proteins in the induced condition underscores the necessity for identifying and characterizing them (Figure 16). For instance, our identification of a calcium-binding mitochondrial protein, facilitated by structural alignment towards the human proteome, led us to the realization that this human homolog is implicated in the bactericidal activity of neutrophils during *Staphylococcus aureus* infection in NETs (Monteith et al., 2022). Although it was differentially expressed in the control condition, contrary to our prediction, our observation sets a precedent for future investigations, suggesting that searching for human structural homologs can illuminate potential proteins associated with ETs.

Regarding the characterized proteins enriched in the induced condition, we found two proteins from the short-chain dehydrogenase/reductase family. These enzymes are present in all life forms (Gabrielli & Tofanelli, 2012) and are involved in redox sensing mechanisms and cellular signaling pathways. Moreover, they are mostly found in the cytoplasm, nucleus,

and mitochondria (Li et al., 2021). These characteristics suggest that these proteins may play a role in *D. discoideum* ETosis. However, further examination is necessary to fully understand their involvement in this process.

The proteomic analysis of the mitochondrial nature of ETs and associated antimicrobial proteins demands further exploration, and the data presented here is not entirely conclusive. However, the differences between both conditions are apparent. Moreover, our study establishes that the fraction under investigation differs from the whole secretome, displaying a lower proportion of unknown proteins than the rest of the proteome. This nuanced insight provides a foundation for future investigations to unravel the specific proteins associated with ETs and their potential implications in the ETosis mechanism, especially when induced by other stimuli such as LPS from *S. enterica*.

4.5 *Dictyostelium discoideum* as an Immune Cell Model

In mammalian immune systems, neutrophils generally sacrifice themselves in producing ETs and working in tandem with phagocytosis to eliminate pathogens. Similarly, phagocytosis is *Dictyostelium's* primary feeding mechanism, and the production of ETs could be a supplementary process to retain bacteria for defense and possibly for nutritional purposes.

This idea aligns with the proposal by Soldati's group, suggesting that converting the constitutive feeding machinery of early free-living eukaryotes into a functional innate immune system is an efficient strategy (Ref Eat, prey Frontiers). In the case of ET from S cells, using ROS as signaling molecules in evolving organisms enabled rapid responses to environmental changes and invasion (Zhang et al., 2016). Thus, the phylogenetic history of

ETosis as a primitive host defense or feeding strategy may explain its paradoxical effects in higher vertebrates (Robb et al., 2014).

Intriguingly, the paradoxical effects between amoeba behavior and immune cells have been reviewed before, extending beyond ETs production. The similarity in phagocytosis, receptor used, chemotaxis, and other immune-like characteristics makes *D. discoideum* a valuable immune cell model (Dunn et al., 2018). Thus, exploring the immune-like characteristics of *D. discoideum* seems to be a promising and exciting research approach.

Using LPS instead of the whole pathogens was a successful approach to decipher differences in the induction of ETs in *D. discoideum* vegetative cells. We determined the proper concentration of induction, kinetics, and timing, and we even visualized ETosis at a single-cell level induced in both conditions. We observed interesting aggregative structures in both strains of *D. discoideum*. Moreover, we determined an enrichment in mtDNA released when induced by LPS with small differences between LPS. Finally, we successfully developed a protocol for studying the global proteomic profile of cells caused by LPS from *K. pneumoniae*, where we identified intriguing differences.

In summary, we propose that vegetative cells of *D. discoideum* offer a promising model for studying ETosis. Investigating this process in a social amoeba, beyond the animal kingdom, could yield valuable insights into its role in bacterial depredation and its mechanistic nature. This approach has the potential to broaden our understanding of complex cellular processes affecting human health. Leveraging our previous knowledge of *D. discoideum* and its practical characteristics, we suggest utilizing it as an immune cell model for studying mammalian innate immunity—akin to Metchnikoff, who used invertebrates to elucidate phagocytosis.

5 CONCLUSIONS

- The production of ETs in vegetative *Dictyostelium discoideum* cells exhibits a dosage-dependent response to induction with LPS from *K. pneumoniae* and *S. enterica*, as demonstrated by microplate reader analysis and live-cell imaging.

- The commitment of cells to ETosis over time varies depending on the LPS used, as indicated by microplate reader analysis and live cell imaging.

- There is a significant increase in mitochondrial DNA within the ET fraction when induced by both LPS from *K. pneumoniae* and *S. enterica*, as revealed by quantitative PCR analysis.

- Notable differences exist between the proteomic profiles of ETs from unstimulated cells and those induced with LPS from *K. pneumoniae*, highlighting the enrichment of unknown proteins and proteins from the short-chain dehydrogenase/reductase family, as demonstrated by mass spectrometry-based proteomics.

- *Dictyostelium discoideum* vegetative cells emerge as a promising model for studying ETosis.

REFERENCES

Atzmony, D., Zahavi, A., & Nanjundiah, V. (1997). Altruistic behaviour in Dictyostelium discoideum explained on the basis of individual selection. *Current Science*, *72*(2), 142-145.

Bateman, A., Martin, M. J., Orchard, S., Magrane, M., Ahmad, S., Alpi, E., Bowler-Barnett, E. H., Britto, R., Bye-A-Jee, H., Cukura, A., Denny, P., Dogan, T., Ebenezer, T. G., Fan, J., Garmiri, P., da Costa Gonzales, L. J., Hatton-Ellis, E., Hussein, A., Ignatchenko, A., … Zhang, J. (2023). UniProt: the Universal Protein Knowledgebase in 2023. *Nucleic Acids Research*, *51*(D1), D523–D531. https://doi.org/10.1093/nar/gkac1052

Benjaminit, Y., & Hochberg, Y. (1995). Controlling the False Discovery Rate: a Practical and Powerful Approach to Multiple Testing. In *J. R. Statist. Soc. B* (Vol. 57, Issue I).

Bloomfield, G., Tanaka, Y., Skelton, J., Ivens, A., & Kay, R. R. (2008). Widespread duplications in the genomes of laboratory stocks of Dictyostelium discoideum. *Genome Biology*, *9*(4). https://doi.org/10.1186/gb-2008-9-4-r75

Bonaventura, A., Vecchié, A., Abbate, A., & Montecucco, F. (2020). Neutrophil Extracellular Traps and Cardiovascular Diseases: An Update. In *Cells* (Vol. 9, Issue 1). NLM (Medline). https://doi.org/10.3390/cells9010231

Bozzaro, S., Bucci, C., & Steinert, M. (2008). Chapter 6 Phagocytosis and Host-Pathogen Interactions in Dictyostelium with a Look at Macrophages. In *International Review of Cell and Molecular Biology* (Vol. 271, Issue C, pp. 253–300). https://doi.org/10.1016/S1937-6448(08)01206-9

Brinkmann, V., Reichard, U., Goosmann, C., Fauler, B., Uhlemann, Y., Weiss, D. S., Weinrauch, Y., & Zychlinsky, A. (2004). *Neutrophil Extracellular Traps Kill Bacteria*. https://www.science.org

Brinkmann, V., & Zychlinsky, A. (2012). Neutrophil extracellular traps: Is immunity the second function of chromatin? In *Journal of Cell Biology* (Vol. 198, Issue 5, pp. 773–783). https://doi.org/10.1083/jcb.201203170

Brock, D. A., Callison, W. É., Strassmann, J. E., & Queller, D. C. (2016). Sentinel cells, symbiotic bacteria and toxin resistance in the social amoeba Dictyostelium discoideum. *Proceedings of the Royal Society B: Biological Sciences*, *283*(1829). https://doi.org/10.1098/rspb.2015.2727

Bronkhorst, A. J., Ungerer, V., Oberhofer, A., Gabriel, S., Polatoglou, E., Randeu, H., Uhlig, C., Pfister, H., Mayer, Z., & Holdenrieder, S. (2022). New Perspectives on the Importance of Cell-Free DNA Biology. In *Diagnostics* (Vol. 12, Issue 9). MDPI. https://doi.org/10.3390/diagnostics12092147

Carmona-Rivera, C., & Kaplan, M. J. (2016). Induction and quantification of NETosis. *Current Protocols in Immunology*, *2016*, 4.41.1-14.41.14. https://doi.org/10.1002/cpim.16

Caroff, M., & Karibian, D. (2003). Structure of bacterial lipopolysaccharides. In *Carbohydrate Research* (Vol. 338, Issue 23, pp. 2431–2447). Elsevier BV. https://doi.org/10.1016/j.carres.2003.07.010

Chapman, E. A., Lyon, M., Simpson, D., Mason, D., Beynon, R. J., Moots, R. J., & Wright, H. L. (2019). Caught in a trap? Proteomic analysis of neutrophil extracellular traps in rheumatoid arthritis and systemic lupus erythematosus. *Frontiers in Immunology*, *10*(MAR). https://doi.org/10.3389/fimmu.2019.00423

Clarke, M., & Maddera, L. (2006). Phagocyte meets prey: Uptake, internalization, and killing of bacteria by Dictyostelium amoebae. *European Journal of Cell Biology*, *85*(9–10), 1001–1010. https://doi.org/10.1016/j.ejcb.2006.05.004

Conceição-Silva, F., Reis, C. S. M., De Luca, P. M., Leite-Silva, J., Santiago, M. A., Morrot, A., & Morgado, F. N. (2021). The immune system throws its traps: Cells and their extracellular traps in disease and protection. In *Cells* (Vol. 10, Issue 8). MDPI. https://doi.org/10.3390/cells10081891

Cubillo-Martínez, A. A., Pereyra, M. A., Garfias, Y., Guluarte, C., Zenteno, E., & Sánchez-Salgado, J. L. (2022). Extracellular traps involved in invertebrate immune mechanisms. In *Fish and Shellfish Immunology* (Vol. 121, pp. 380–386). Academic Press. https://doi.org/10.1016/j.fsi.2022.01.024

Damascena, H. L., Silveira, W. A. A., Castro, M. S., & Fontes, W. (2022). Neutrophil Activated by the Famous and Potent PMA (Phorbol Myristate Acetate). In *Cells* (Vol. 11, Issue 18). MDPI. https://doi.org/10.3390/cells11182889

Daniel, C., Leppkes, M., Muñoz, L. E., Schley, G., Schett, G., & Herrmann, M. (2019). Extracellular DNA traps in inflammation, injury and healing. In *Nature Reviews Nephrology* (Vol. 15, Issue 9, pp. 559–575). Nature Publishing Group. https://doi.org/10.1038/s41581-019-0163-2

Dormann, D., Vasiev, B., & Weijer, C. J. (2002). Becoming Multicellular by Aggregation; The Morphogenesis of the Social Amoebae Dicyostelium discoideum. In *Journal of Biological Physics* (Vol. 28).

Dunn, J. D., Bosmani, C., Barisch, C., Raykov, L., Lefrançois, L. H., Cardenal-Muñoz, E., López-Jiménez, A. T., & Soldati, T. (2018). Eat prey, live: Dictyostelium discoideum as

a model for cell-autonomous defenses. In *Frontiers in Immunology* (Vol. 8, Issue JAN). Frontiers Media S.A. https://doi.org/10.3389/fimmu.2017.01906

Escalante, R., & Cardenal-Muñoz, E. (2019). Preface: Dictyostelium discoideum: The organism and the model. In *International Journal of Developmental Biology* (Vol. 63, Issues 9–10, pp. 317–320). University of the Basque Country Press. https://doi.org/10.1387/ijdb.190275re

Farías-Moreno, S., & Chavez Espinosa, F. (2021). *Estudio de la dinámica de interacción entre Dictyostelium discoideum y Klebsiella pneumoniae mediante microscopía automática de fluorescencia* [University of Chile]. https://repositorio.uchile.cl/handle/2250/184864

Freitas, A. V., Herb, J. T., Pan, M., Chen, Y., Gucek, M., Jin, T., & Xu, H. (2022). Generation of a mitochondrial protein compendium in Dictyostelium discoideum. *IScience*, *25*(5). https://doi.org/10.1016/j.isci.2022.104332

Fuchs, T. A., Abed, U., Goosmann, C., Hurwitz, R., Schulze, I., Wahn, V., Weinrauch, Y., Brinkmann, V., & Zychlinsky, A. (2007). Novel cell death program leads to neutrophil extracellular traps. *Journal of Cell Biology*, *176*(2), 231–241. https://doi.org/10.1083/jcb.200606027

Gabrielli, F., & Tofanelli, S. (2012). Molecular and functional evolution of human DHRS2 and DHRS4 duplicated genes. *Gene*, *511*(2), 461–469. https://doi.org/10.1016/j.gene.2012.09.013

Gao, C. H., Yu, G., & Cai, P. (2021). ggVennDiagram: An Intuitive, Easy-to-Use, and Highly Customizable R Package to Generate Venn Diagram. *Frontiers in Genetics*, *12*. https://doi.org/10.3389/fgene.2021.706907

Gavillet, M., Martinod, K., Renella, R., Harris, C., Shapiro, N. I., Wagner, D. D., & Williams, D. A. (2015). Flow cytometric assay for direct quantification of neutrophil extracellular traps in blood samples. *American Journal of Hematology*, *90*(12), 1155–1158. https://doi.org/10.1002/ajh.24185

G.E. Truett, P. Heeger, R.L. Mynatt, A.A. Truett, J.A. Walker, & M.L. Warman. (2000). Preparation of PCR-Quality Mouse Genomic DNA with Hot Sodium Hydroxide and Tris (HotSHOT). *Bioechniques*, *29*, 52–54.

Goldberg, J. M., Manning, G., Liu, A., Fey, P., Pilcher, K. E., Xu, Y., & Smith, J. L. (2006). The Dictyostelium kinome - Analysis of the protein kinases from a simple model organism. *PLoS Genetics*, *2*(3), 0291–0303. https://doi.org/10.1371/journal.pgen.0020038

Goldmann, O., & Medina, E. (2012). The expanding world of extracellular traps: Not only neutrophils but much more. In *Frontiers in Immunology* (Vol. 3, Issue JAN). https://doi.org/10.3389/fimmu.2012.00420

Gu, Z., Eils, R., & Schlesner, M. (2016). Complex heatmaps reveal patterns and correlations in multidimensional genomic data. *Bioinformatics*, *32*(18), 2847–2849. https://doi.org/10.1093/bioinformatics/btw313

Guimarães-Costa, A. B., Nascimento, M. T. C., Wardini, A. B., Pinto-Da-Silva, L. H., & Saraiva, E. M. (2012). ETosis: A microbicidal mechanism beyond cell death. In *Journal of Parasitology Research* (Vol. 2012). https://doi.org/10.1155/2012/929743

Henneck, T., Krüger, C., Nerlich, A., Langer, M., Fingerhut, L., Bonilla, M. C., Meurer, M., von den Berg, S., de Buhr, N., Branitzki-Heinemann, K., & von Köckritz-Blickwede, M. (2023). Comparison of NET quantification methods based on immunofluorescence

microscopy: Hand-counting, semi-automated and automated evaluations. *Heliyon*, *9*(6). https://doi.org/10.1016/j.heliyon.2023.e16982

Hernández, M., Areche, C., Castañeta, G., Rojas, D., Varas, M. A., Marcoleta, A. E., & Chávez, F. P. (2023). *Dictyostelium discoideum-assisted pharmacognosy of plant resources for discovering antivirulence molecules targeting Klebsiella pneumoniae*. https://doi.org/10.1101/2023.10.27.564015

Homa, J. (2018). Earthworm coelomocyte extracellular traps: structural and functional similarities with neutrophil NETs. In *Cell and Tissue Research* (Vol. 371, Issue 3, pp. 407–414). Springer Verlag. https://doi.org/10.1007/s00441-018-2787-0

Homa, J., Ortmann, W., & Kolaczkowska, E. (2016). Conservative mechanisms of extracellular trap formation by annelida eisenia andrei: Serine protease activity requirement. *PLoS ONE*, *11*(7). https://doi.org/10.1371/journal.pone.0159031

Hoppenbrouwers, T., Autar, A. S. A., Sultan, A. R., Abraham, T. E., Van Cappellen, W. A., Houtsmuller, A. B., Van Wamel, W. J. B., Van Beusekom, H. M. M., Van Neck, J. W., & De Maat, M. P. M. (2017). In vitro induction of NETosis: Comprehensive live imaging comparison and systematic review. *PLoS ONE*, *12*(5). https://doi.org/10.1371/journal.pone.0176472

J. Hahn, J. Knopf, C. Maueröder, D. Kienhöfer, M. Leppkes, & M. Herrmann. (2016). Neutrophils and neutrophil extracellular traps orchestrate initiation and resolution of inflammation. *Clin Exp Rheumatol*, *34*, S6–S8.

Jumper, J., Evans, R., Pritzel, A., Green, T., Figurnov, M., Ronneberger, O., Tunyasuvunakool, K., Bates, R., Žídek, A., Potapenko, A., Bridgland, A., Meyer, C., Kohl, S. A. A., Ballard, A. J., Cowie, A., Romera-Paredes, B., Nikolov, S., Jain, R.,

Adler, J., … Hassabis, D. (2021). Highly accurate protein structure prediction with AlphaFold. *Nature*, *596*(7873), 583–589. https://doi.org/10.1038/s41586-021-03819-2

Junemann, A., Filić, V., Winterhoff, M., Nordholz, B., Litschko, C., Schwellenbach, H., Stephan, T., Weber, I., & Faix, J. (2016). A Diaphanous-related formin links Ras signaling directly to actin assembly in macropinocytosis and phagocytosis. *Proceedings of the National Academy of Sciences of the United States of America*, *113*(47), E7464–E7473. https://doi.org/10.1073/pnas.1611024113

Kamoshida, G., Kikuchi-Ueda, T., Nishida, S., Tansho-Nagakawa, S., Kikuchi, H., Ubagai, T., & Ono, Y. (2017). Spontaneous formation of neutrophil extracellular traps in serum-free culture conditions. *FEBS Open Bio*, *7*(6), 877–886. https://doi.org/10.1002/2211-5463.12222

Kaplan, M. J., & Radic, M. (2012). Neutrophil Extracellular Traps: Double-Edged Swords of Innate Immunity. *The Journal of Immunology*, *189*(6), 2689–2695. https://doi.org/10.4049/jimmunol.1201719

Kaufmann, S. H. E. (2008). Immunology's foundation: the 100-year anniversary of the Nobel Prize to Paul Ehrlich and Elie Metchnikoff. *Nature Immunology*, *9*(7), 705–712. https://www.nature.com/articles/ni0708-705

Kenny, E. F., Herzig, A., Krüger, R., Muth, A., Mondal, S., Thompson, P. R., Brinkmann, V., Bernuth, H. von, & Zychlinsky, A. (2017). Diverse stimuli engage different neutrophil extracellular trap pathways. *ELife*, *6*. https://doi.org/10.7554/eLife.24437

Kong, A. T., Leprevost, F. V., Avtonomov, D. M., Mellacheruvu, D., & Nesvizhskii, A. I. (2017). MSFragger: Ultrafast and comprehensive peptide identification in mass spectrometry-based proteomics. *Nature Methods*, *14*(5), 513–520. https://doi.org/10.1038/nmeth.4256

Kreppel, L., Fey, P., Gaudet, P., Just, E., Kibbe, W. A., Chisholm, R. L., & Kimmel, A. R. (2004). dictyBase: A new Dictyostelium discoideum genome database. *Nucleic Acids Research*, *32*(DATABASE ISS.). https://doi.org/10.1093/nar/gkh138

Lamrabet, O., Melotti, A., Burdet, F., Hanna, N., Perrin, J., Nitschke, J., Pagni, M., Hilbi, H., Soldati, T., & Cosson, P. (2020). Transcriptional Responses of Dictyostelium discoideum Exposed to Different Classes of Bacteria. *Frontiers in Microbiology*, *11*. https://doi.org/10.3389/fmicb.2020.00410

Leppkes, M., Maueröder, C., Hirth, S., Nowecki, S., Günther, C., Billmeier, U., Paulus, S., Biermann, M., Munoz, L. E., Hoffmann, M., Wildner, D., Croxford, A. L., Waisman, A., Mowen, K., Jenne, D. E., Krenn, V., Mayerle, J., Lerch, M. M., Schett, G., … Becker, C. (2016). Externalized decondensed neutrophil chromatin occludes pancreatic ducts and drives pancreatitis. *Nature Communications*, *7*. https://doi.org/10.1038/ncomms10973

Li, Z., Liu, H., Bode, A., & Luo, X. (2021). Emerging roles of dehydrogenase/reductase member 2 (DHRS2) in the pathology of disease. In *European Journal of Pharmacology* (Vol. 898). Elsevier B.V. https://doi.org/10.1016/j.ejphar.2021.173972

Liu, S., Su, X., Pan, P., Zhang, L., Hu, Y., Tan, H., Wu, D., Liu, B., Li, H., Li, H., Li, Y., Dai, M., Li, Y., Hu, C., & Tsung, A. (2016). Neutrophil extracellular traps are indirectly triggered by lipopolysaccharide and contribute to acute lung injury. *Scientific Reports*, *6*. https://doi.org/10.1038/srep37252

Marcoleta, A. E., Varas, M. A., Ortiz-Severín, J., Vásquez, L., Berríos-Pastén, C., Sabag, A. V., Chávez, F. P., Allende, M. L., Santiviago, C. A., Monasterio, O., & Lagos, R. (2018). Evaluating different virulence traits of Klebsiella pneumoniae using Dictyostelium

discoideum and zebrafish larvae as host models. *Frontiers in Cellular and Infection Microbiology*, *8*(FEB). https://doi.org/10.3389/fcimb.2018.00030

Mathavarajah, S., Flores, A., & Huber, R. J. (2017). Dictyostelium discoideum: A Model System for Cell and Developmental Biology. *Current Protocols in Essential Laboratory Techniques*, *15*(1), 14.1.1-14.1.19. https://doi.org/10.1002/cpet.15

Metschnikoff, E. (1878). -. *Zoologischer Anzeiger*, *1*, 387–394.

Metschnikoff, E. (1880). -. *Zoologischer Anzeiger*, *3*, 261–263.

Metschnikoff, E. (1884a). -. *Arb. Zool. Inst. Univ. Wien. u. Zool. Stat. Triest*, *5*, 141–168.

Metschnikoff, E. (1884b). -. *Virchows Arch*, *96*, 177–195.

Monteith, A. J., Miller, J. M., Beavers, W. N., Maloney, K. N., Seifert, E. L., Hajnoczky, G., & Skaar, E. P. (2022). *Mitochondrial Calcium Uniporter Affects Neutrophil Bactericidal Activity during Staphylococcus aureus Infection*. https://journals.asm.org/journal/iai

Morshed, M., Hlushchuk, R., Simon, D., Walls, A. F., Obata-Ninomiya, K., Karasuyama, H., Djonov, V., Eggel, A., Kaufmann, T., Simon, H.-U., & Yousefi, S. (2014). NADPH Oxidase–Independent Formation of Extracellular DNA Traps by Basophils. *The Journal of Immunology*, *192*(11), 5314–5323. https://doi.org/10.4049/jimmunol.1303418

Naccache, P. H., & Fernandes, M. J. G. (2016). Challenges in the characterization of neutrophil extracellular traps: The truth is in the details. *European Journal of Immunology*, *46*(1), 52–55. https://doi.org/10.1002/eji.201546022

Nakazawa, D., Marschner, J. A., Platen, L., & Anders, H. J. (2018). Extracellular traps in kidney disease. In *Kidney International* (Vol. 94, Issue 6, pp. 1087–1098). Elsevier B.V. https://doi.org/10.1016/j.kint.2018.08.035

Nasser, W., Santhanam, B., Miranda, E. R., Parikh, A., Juneja, K., Rot, G., Dinh, C., Chen, R., Zupan, B., Shaulsky, G., & Kuspa, A. (2013). Bacterial discrimination by

dictyostelid amoebae reveals the complexity of ancient interspecies interactions. *Current Biology*, *23*(10), 862–872. https://doi.org/10.1016/j.cub.2013.04.034

Neumann, A., Brogden, G., & von Köckritz-Blickwede, M. (2020). Extracellular traps: An ancient weapon of multiple kingdoms. In *Biology* (Vol. 9, Issue 2). MDPI AG. https://doi.org/10.3390/biology9020034

Ng, T. H., Chang, S. H., Wu, M. H., & Wang, H. C. (2013). Shrimp hemocytes release extracellular traps that kill bacteria. *Developmental and Comparative Immunology*, *41*(4), 644–651. https://doi.org/10.1016/j.dci.2013.06.014

Papayannopoulos, V. (2018). Neutrophil extracellular traps in immunity and disease. In *Nature Reviews Immunology* (Vol. 18, Issue 2, pp. 134–147). Nature Publishing Group. https://doi.org/10.1038/nri.2017.105

Papayannopoulos, V., Metzler, K. D., Hakkim, A., & Zychlinsky, A. (2010). Neutrophil elastase and myeloperoxidase regulate the formation of neutrophil extracellular traps. *Journal of Cell Biology*, *191*(3), 677–691. https://doi.org/10.1083/jcb.201006052

Petretto, A., Bruschi, M., Pratesi, F., Croia, C., Candiano, G., Ghiggeri, G., & Migliorini, P. (2019). Neutrophil extracellular traps (NET) induced by different stimuli: A comparative proteomic analysis. *PLoS ONE*, *14*(7). https://doi.org/10.1371/journal.pone.0218946

Pieterse, E., Rother, N., Yanginlar, C., Hilbrands, L. B., & van der Vlag, J. (2016). Neutrophils discriminate between lipopolysaccharides of different bacterial sources and selectively release neutrophil extracellular traps. *Frontiers in Immunology*, *7*(NOV). https://doi.org/10.3389/fimmu.2016.00484

Pilsczek, F. H., Salina, D., Poon, K. K. H., Fahey, C., Yipp, B. G., Sibley, C. D., Robbins, S. M., Green, F. H. Y., Surette, M. G., Sugai, M., Bowden, M. G., Hussain, M., Zhang, K.,

& Kubes, P. (2010). A Novel Mechanism of Rapid Nuclear Neutrophil Extracellular Trap Formation in Response to Staphylococcus aureus . *The Journal of Immunology*, *185*(12), 7413–7425. https://doi.org/10.4049/jimmunol.1000675

Porto, B. N., & Stein, R. T. (2016). Neutrophil extracellular traps in pulmonary diseases: Too much of a good thing? *Frontiers in Immunology*, *7*(AUG). https://doi.org/10.3389/fimmu.2016.00311

Poto, R., Cristinziano, L., Modestino, L., de Paulis, A., Marone, G., Loffredo, S., Galdiero, M. R., & Varricchi, G. (2022). Neutrophil Extracellular Traps, Angiogenesis and Cancer. In *Biomedicines* (Vol. 10, Issue 2). MDPI. https://doi.org/10.3390/biomedicines10020431

Raetz, C. R. H., & Whitfield, C. (2002). Lipopolysaccharide endotoxins. In *Annual Review of Biochemistry* (Vol. 71, pp. 635–700). https://doi.org/10.1146/annurev.biochem.71.110601.135414

Rafia, S., & Saran, S. (2019). Sestrin-like protein from Dictyostelium discoideum is involved in autophagy under starvation stress. *Microbiological Research*, *220*, 61–71. https://doi.org/10.1016/j.micres.2018.12.006

Raper KB. (1935). Dictyostelium discoideum, A new species of slime mold from decaying forest leaves. *J Agric Res*, *50*, 135–147.

Rietschel, E. T., Ki, T., Shade, T., MAMAi, U., Scrmhy, N., Loepno, H. A., Ulmer, U., Zhrjner, U., Seydel, U., & PAVA MAXSCfl E AND HELMUT BRADE, F. DI. (1994). Bacterial endotoxin: molecular relationships of structure to activity and function. *The FASEB Journal*, *8*(2), 217–225. www.fasebj.org

Robb, C. T., Dyrynda, E. A., Gray, R. D., Rossi, A. G., & Smith, V. J. (2014). Invertebrate extracellular phagocyte traps show that chromatin is an ancient defence weapon. *Nature Communications*, *5*. https://doi.org/10.1038/ncomms5627

Scavello, M., Petlick, A. R., Ramesh, R., Thompson, V. F., Lotfi, P., & Charest, P. G. (2017). Protein kinase A regulates the Ras, Rap1 and TORC2 pathways in response to the chemoattractant cAMP in Dictyostelium. *Journal of Cell Science*, *130*(9), 1545–1558. https://doi.org/10.1242/jcs.177170

Schauer, C., Janko, C., Munoz, L. E., Zhao, Y., Kienhöfer, D., Frey, B., Lell, M., Manger, B., Rech, J., Naschberger, E., Holmdahl, R., Krenn, V., Harrer, T., Jeremic, I., Bilyy, R., Schett, G., Hoffmann, M., & Herrmann, M. (2014). Aggregated neutrophil extracellular traps limit inflammation by degrading cytokines and chemokines. *Nature Medicine*, *20*(5), 511–517. https://doi.org/10.1038/nm.3547

Schorn, C., Janko, C., Latzko, M., Chaurio, R., Schett, G., & Herrmann, M. (2012). Monosodium urate crystals induce extracellular DNA traps in neutrophils, eosinophils, and basophils but not in mononuclear cells. *Frontiers in Immunology*, *3*(SEP). https://doi.org/10.3389/fimmu.2012.00277

Scieszka, D., Lin, Y. H., Li, W., Choudhury, S., Yu, Y., & Freire, M. (2022). NETome: A model to Decode the Human Genome and Proteome of Neutrophil Extracellular Traps. *Scientific Data*, *9*(1). https://doi.org/10.1038/s41597-022-01798-1

Steimle, A., Autenrieth, I. B., & Frick, J. S. (2016). Structure and function: Lipid A modifications in commensals and pathogens. In *International Journal of Medical Microbiology* (Vol. 306, Issue 5, pp. 290–301). Elsevier GmbH. https://doi.org/10.1016/j.ijmm.2016.03.001

Steinert, M., & Heuner, K. (2005). Dictyostelium as host model for pathogenesis. In *Cellular Microbiology* (Vol. 7, Issue 3, pp. 307–314). https://doi.org/10.1111/j.1462-5822.2005.00493.x

Thomas, P. D., Ebert, D., Muruganujan, A., Mushayahama, T., Albou, L. P., & Mi, H. (2022). PANTHER: Making genome-scale phylogenetics accessible to all. In *Protein Science* (Vol. 31, Issue 1, pp. 8–22). John Wiley and Sons Inc. https://doi.org/10.1002/pro.4218

Urban, C. F., Ermert, D., Schmid, M., Abu-Abed, U., Goosmann, C., Nacken, W., Brinkmann, V., Jungblut, P. R., & Zychlinsky, A. (2009). Neutrophil extracellular traps contain calprotectin, a cytosolic protein complex involved in host defense against Candida albicans. *PLoS Pathogens*, *5*(10). https://doi.org/10.1371/journal.ppat.1000639

Urban, C. F., Reichard, U., Brinkmann, V., & Zychlinsky, A. (2006). Neutrophil extracellular traps capture and kill Candida albicans and hyphal forms. *Cellular Microbiology*, *8*(4), 668–676. https://doi.org/10.1111/j.1462-5822.2005.00659.x

van Kempen, M., Kim, S. S., Tumescheit, C., Mirdita, M., Lee, J., Gilchrist, C. L. M., Söding, J., & Steinegger, M. (2023). Fast and accurate protein structure search with Foldseek. *Nature Biotechnology*. https://doi.org/10.1038/s41587-023-01773-0

Varas, M. A., Riquelme-Barrios, S., Valenzuela, C., Marcoleta, A. E., Berríos-Pastén, C., Santiviago, C. A., & Chávez, F. P. (2018). Inorganic polyphosphate is essential for Salmonella Typhimurium Virulence and survival in Dictyostelium discoideum. *Frontiers in Cellular and Infection Microbiology*, *8*(JAN). https://doi.org/10.3389/fcimb.2018.00008

Vinogradov, E., Frirdich, E., MacLean, L. L., Perry, M. B., Petersen, B. O., Duus, J., & Whitfield, C. (2002). Structures of lipopolysaccharides from Klebsiella pneumoniae: Elucidation of the structure of the linkage region between core and polysaccharide O

chain and identification of the residues at the non-reducing termini of the O chains. *Journal of Biological Chemistry*, *277*(28), 25070–25081. https://doi.org/10.1074/jbc.M202683200

Von Köckritz-Blickwede, M., Goldmann, O., Thulin, P., Heinemann, K., Norrby-Teglund, A., Rohde, M., & Medina, E. (2008). Phagocytosis-independent antimicrobial activity of mast cells by means of extracellular trap formation. *Blood*, *111*(6), 3070–3080. https://doi.org/10.1182/blood-2007-07-104018

Wang, X., Zhao, J., Cai, C., Tang, X., Fu, L., Zhang, A., & Han, L. (2018). A label-free quantitative proteomic analysis of mouse neutrophil extracellular trap formation induced by streptococcus suisor phorbol myristate acetate (PMA). *Frontiers in Immunology*, *9*(NOV). https://doi.org/10.3389/fimmu.2018.02615

Wang Xiaoyuan, & Quinn Peter J. (2010). Endotoxins: Structure, Function and Recognition. In *Endotoxins: Structure, Function and Recognition* (Vol. 53, pp. 3–25).

Wang, Y., Li, M., Stadler, S., Correll, S., Li, P., Wang, D., Hayama, R., Leonelli, L., Han, H., Grigoryev, S. A., Allis, C. D., & Coonrod, S. A. (2009). Histone hypercitrullination mediates chromatin decondensation and neutrophil extracellular trap formation. *Journal of Cell Biology*, *184*(2), 205–213. https://doi.org/10.1083/jcb.200806072

Wickham, H., Averick, M., Bryan, J., Chang, W., McGowan, L., François, R., Grolemund, G., Hayes, A., Henry, L., Hester, J., Kuhn, M., Pedersen, T., Miller, E., Bache, S., Müller, K., Ooms, J., Robinson, D., Seidel, D., Spinu, V., … Yutani, H. (2019). Welcome to the Tidyverse. *Journal of Open Source Software*, *4*(43), 1686. https://doi.org/10.21105/joss.01686

Yipp, B. G., Petri, B., Salina, D., Jenne, C. N., Scott, B. N. V., Zbytnuik, L. D., Pittman, K., Asaduzzaman, M., Wu, K., Meijndert, H. C., Malawista, S. E., De Boisfleury Chevance,

A., Zhang, K., Conly, J., & Kubes, P. (2012). Infection-induced NETosis is a dynamic process involving neutrophil multitasking in vivo. *Nature Medicine*, *18*(9), 1386–1393. https://doi.org/10.1038/nm.2847

Yousefi, S., Gold, J. A., Andina, N., Lee, J. J., Kelly, A. M., Kozlowski, E., Schmid, I., Straumann, A., Reichenbach, J., Gleich, G. J., & Simon, H. U. (2008). Catapult-like release of mitochondrial DNA by eosinophils contributes to antibacterial defense. *Nature Medicine*, *14*(9), 949–953. https://doi.org/10.1038/nm.1855

Yousefi, S., Mihalache, C., Kozlowski, E., Schmid, I., & Simon, H. U. (2009). Viable neutrophils release mitochondrial DNA to form neutrophil extracellular traps. *Cell Death and Differentiation*, *16*(11), 1438–1444. https://doi.org/10.1038/cdd.2009.96

Yousefi, S., Stojkov, D., Germic, N., Simon, D., Wang, X., Benarafa, C., & Simon, H. U. (2019). Untangling "NETosis" from NETs. In *European Journal of Immunology* (Vol. 49, Issue 2, pp. 221–227). Wiley-VCH Verlag. https://doi.org/10.1002/eji.201747053

Zenk, S. F., Jantsch, J., & Hensel, M. (2009). Role of Salmonella enterica Lipopolysaccharide in Activation of Dendritic Cell Functions and Bacterial Containment . *The Journal of Immunology*, *183*(4), 2697–2707. https://doi.org/10.4049/jimmunol.0900937

Zhang, X., Zhuchenko, O., Kuspa, A., & Soldati, T. (2016). Social amoebae trap and kill bacteria by casting DNA nets. *Nature Communications*, *7*. https://doi.org/10.1038/ncomms10938

Zhu, L., Liu, L., Zhang, Y., Pu, L., Liu, J., Li, X., Chen, Z., Hao, Y., Wang, B., Han, J., Li, G., Liang, S., Xiong, H., Zheng, H., Li, A., Xu, J., & Zeng, H. (2018). High Level of Neutrophil Extracellular Traps Correlates with Poor Prognosis of Severe Influenza A Infection. *Journal of Infectious Diseases*, *217*(3), 428–437. https://doi.org/10.1093/infdis/jix475

ANNEX

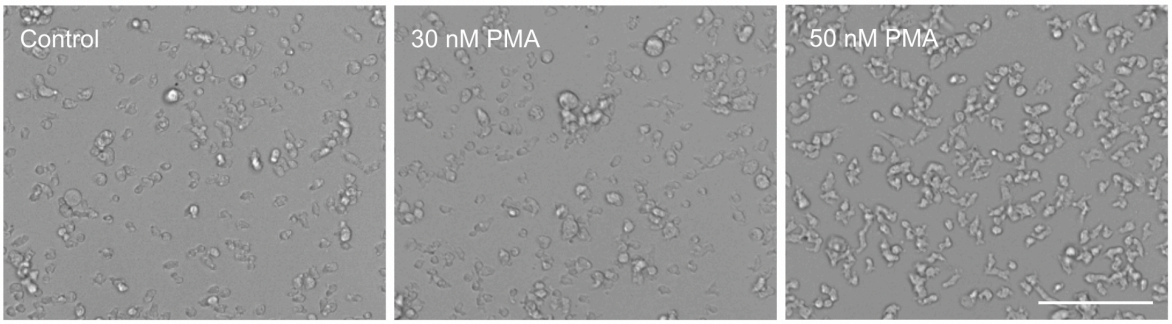

Supplementary Figure 1. AX4 cells induce with PMA for 4 hours. Cells were seeded in a 24-well plate at described with different concentration of PMA in visualized in bright field. Scale bar: 100µm

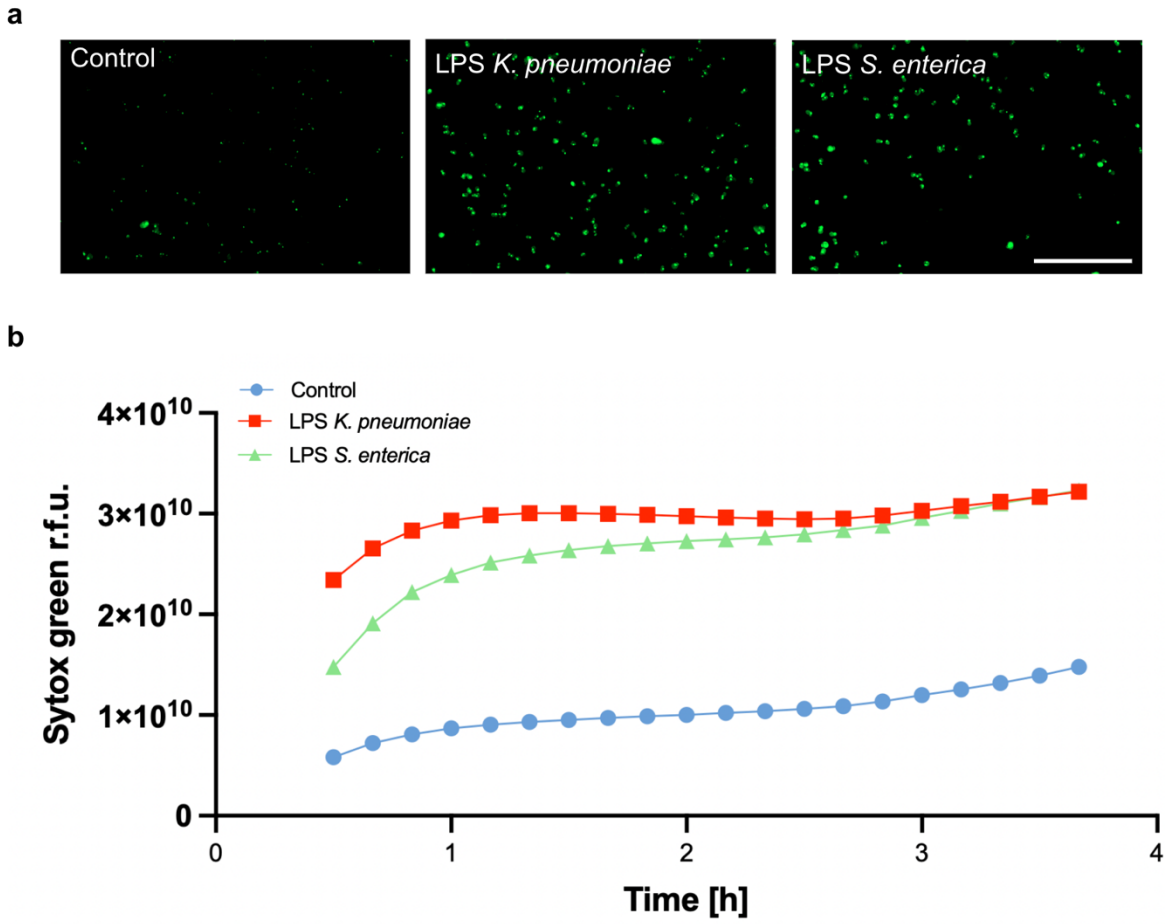

Supplementary Figure 2. Extracellular Trap Release Measured by Automated Fluorescent Microscopy Using Sytox Green Fluorescence. a) Representative images of the area measured after 4 hours of induction b) Sytox green fluorescence over time. The measurements were conducted using sytox green fluorescence, with the surface center of the plate captured, encompassing between 150-200 cells per condition. To achieve this, a stitching of four 20X amplification images forming a montage was performed. Scale bar: 200 µm.

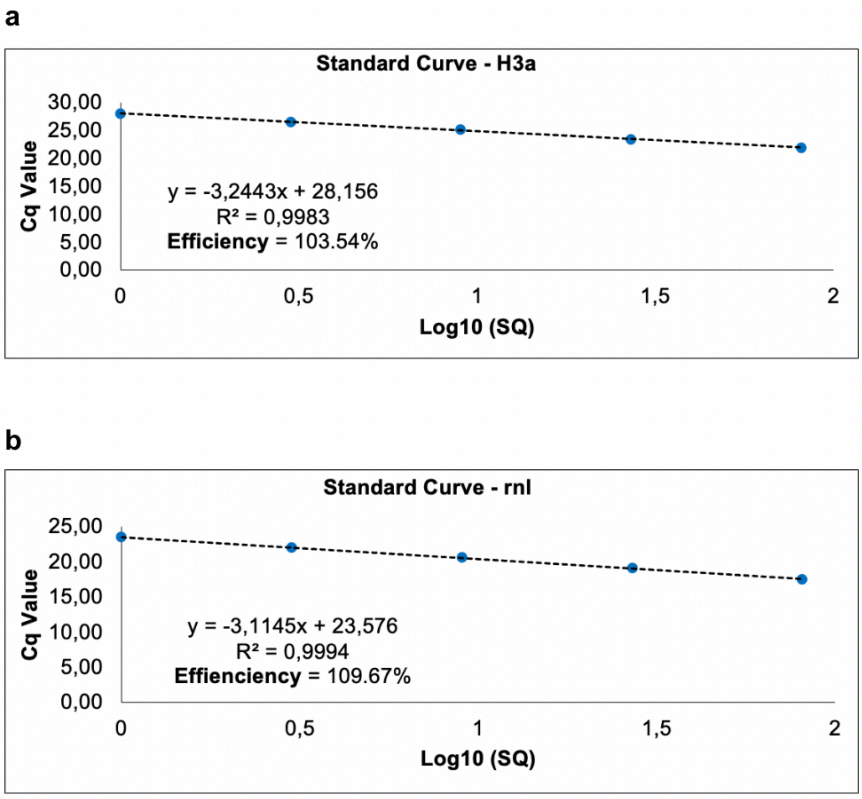

Supplementary Figure 3. Standard Curve of a) Nuclear and b) Mitochondrial Primers. Different dilutions from purified genomic DNA of *D. dictyostelium* were used as templates, and the PCR amplifications were performed in triplicates for both nuclear (top) and mitochondrial (bottom) primers. Efficiency was calculated for each primer.

Supplementary Table 1. Protocol comparison for NET proteins isolation

Steps	Urban 2009	Chapman 2019	Petretto 2019	Steps	Scieszka 2022
Cell Source	Human neutrophils	Human Neutrophils	Human Neutrophils		Neutrophils differentiated from HL-60 cell line
Induction Stimuli	a) 20 nM PMA -Time: 4 hours	a) 50 nM PMA b) 3.8µM A23187 -Time: 4 hours	a) 100 nM PMA b) 4 µM A23187 c) 1 µg/ml LPS from *E. coli* -Time: 3 hours		a) 1000 nM PMA -Time: 4 hours
Cell Incubation	-Seeded in 12-well plates. -Concentration: 1.7×10^6 cell/ml	-Seeded in 12-well plates. -Concentration: 1.7×10^6 cell/ml	-Seeded in 10mm Petri dishes -Concentration: 10×10^6 cells/plate		-Seeded in 150 x 25mm flat dish. -Concentration: 5×10^6 cells/ml.
Media removal	-Cell media aspirated. -Cell washed twice for 10 minutes by pipetting 1 ml of fresh and pre-warmed RPMI.	-Cell media aspirated. -Cells washed twice for 10 minutes with RPMI media (no serum).	-Cell media aspirated. -Cells washed twice for 10 minutes with 10 mL of Dulbecco-modified phosphate buffer saline.		-Cell media aspirated. -Attached cells were resuspended in ice-cold PBS.
Nuclease Treatment	-1 mL RPMI media with 10 U/ml DNase-1 for 20 minutes. -Reaction stopped with 5 mM EDTA (final concentration).	-1 mL RPMI media with 1µM CaCl2 and 50 mU. micrococcal nuclease for 20 minutes. -Reaction stopped with 5 µM EDTA (final concentration).	- HBSS with CaCl2 2 mM and 10 U/ml DNase I for 20 minutes. -Reaction stopped with 5 mM EDTA (final concentration).	**Protein Precipitation**	- Samples were then centrifuged at 275 x g for 10 minutes. -DNA-rich supernatant was centrifugated at 18,000 × g for 10 minutes at RT. -Supernatant was aspirated. -DNA pellets were resuspended for storage.
Protein Precipitation	-Samples were then centrifugated at 300 x g -DNA-rich supernatant was then centrifugated at 16,000x g. -Supernatant containing NET proteins was precipitated with acetone and digest for LC-MS/MS analysis.	-Digested NET material was removed by gently tilting the plate and removing the supernatant. - Supernatant was then centrifuged at 400 x g for 5 minutes at 4°C -DNA-rich supernatant was carefully transferred to a clean tube and centrifuged at 16,000 g for 5 min at 4 °C. -Supernatant containing NET proteins was precipitated using Strata clean beads and then digested for LC-MS/MS analysis.	-Samples were then centrifuged 10' at 3000g. -Supernatant containing NET proteins was precipitated with acetone and then digested for LC-MS/MS analysis.	**Nuclease Treatment**	-Solution containing NETs was then treated with 1% Benzonase Nuclease and incubated for 20 minutes. -Suspension Trapping approach was used for LC-MS/MS analysis.

Supplementary Table 2. Primer sequences used.

Name	Sequence
rnl-F	TGATCCAATAGTTCTGTGTGGA
rnl-R	CCGAACCACATAACAGATATGA
H3a-F	GGTTCTAAACAAGCCCATAAACA
H3a-R	CTCTAAGAGCGACAGTAC